AD-A099 714 ARMY ELECTRONICS RESEARCH AND DEVELOPMENT COMMAND FO--ETC F/G 9/1
CIRCUITLESS ELECTRON BEAM AMPLIFIER (CEBA).(U)
MAR 81 L J JASPER, C M DE SANTIS

UNCLASSIFIED DELET-TR-81-8 NL

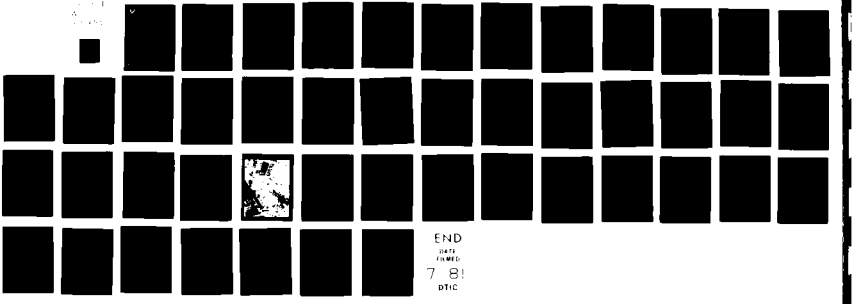

END
DATE FILMED
7 81
DTIC

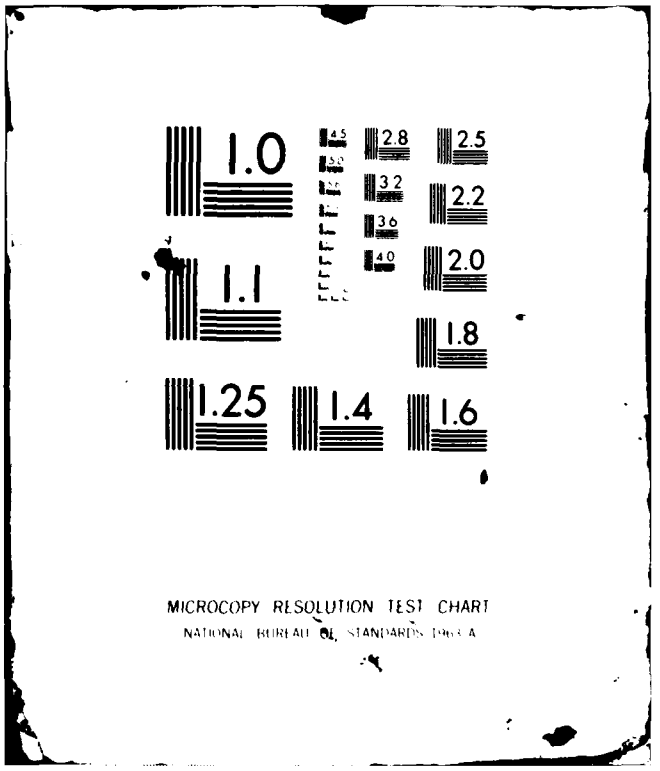
1.0
1.1
1.25
1.4
1.6
1.8
2.0
2.2
2.5
2.8
3.2
3.6
4.0
4.5
5.0
MICROCOPY RESOLUTION TEST CHART
NATIONAL BUREAU OF STANDARDS 1963-A

LEVEL II (12)

RESEARCH AND DEVELOPMENT TECHNICAL REPORT

DELET-TR-81-8

CIRCUITLESS ELECTRON BEAM AMPLIFIER (CEBA)

L. J. JASPER, JR.
C. M. DE SANTIS
ELECTRONICS TECHNOLOGY & DEVICES LABORATORY

MARCH 1981

DISTRIBUTION STATEMENT
Approved for public release;
distribution unlimited.

ERADCOM
US ARMY ELECTRONICS RESEARCH & DEVELOPMENT COMMAND
FORT MONMOUTH, NEW JERSEY 07703

NOTICES

Disclaimers

The citation of trade names and names of manufacturers in this report is not to be construed as official Government indorsement or approval of commercial products or services referenced herein.

Disposition

Destroy this report when it is no longer needed. Do not return it to the originator.

UNCLASSIFIED

SECURITY CLASSIFICATION OF THIS PAGE (When Data Entered)

(14) REPORT DOCUMENTATION PAGE		READ INSTRUCTIONS BEFORE COMPLETING FORM
1. REPORT NUMBER DELET-TR- 81-8	2. GOVT ACCESSION NO. AD-A099 724	3. RECIPIENT'S CATALOG NUMBER
4. TITLE (and Subtitle) (6) CIRCUITLESS ELECTRON BEAM AMPLIFIER (CEBA),		5. TYPE OF REPORT & PERIOD COVERED (9) Technical Report,
		6. PERFORMING ORG. REPORT NUMBER
7. AUTHOR(s) (10) L. J. Jasper, Jr. C. M. De Santis		8. CONTRACT OR GRANT NUMBER(s)
9. PERFORMING ORGANIZATION NAME AND ADDRESS USA Electronics Technology & Devices Lab., ERADCOM, Fort Monmouth, New Jersey 07703 (16)		10. PROGRAM ELEMENT, PROJECT, TASK AREA & WORK UNIT NUMBERS (17) 1L1 62705AH94 01 02
11. CONTROLLING OFFICE NAME AND ADDRESS Beam, Plasma & Display Division US Army Electronics Technology & Devices Lab (ERADCOM) ATTN: DELET-BM, Ft Mon, NJ 07703		12. REPORT DATE (11) Mar[redacted]81 13. NUMBER OF PAGES 41 (12) 47
14. MONITORING AGENCY NAME & ADDRESS (if different from Controlling Office)		15. SECURITY CLASS. (of this report) Unclassified 15a. DECLASSIFICATION/DOWNGRADING SCHEDULE

16. DISTRIBUTION STATEMENT (of this Report)

Approved for public release; distribution unlimited

17. DISTRIBUTION STATEMENT (of the abstract entered in Block 20, if different from Report)

18. SUPPLEMENTARY NOTES

19. KEY WORDS (Continue on reverse side if necessary and identify by block number)

Microwave tube
Millimeter tube
Electron Beam Amplifier
Amplication of electromagnetic waves
Traveling-wave tube
Microwave/Millimeter wave amplifier
Active Dielectric Medium

20. ABSTRACT (Continue on reverse side if necessary and identify by block number)

A study is presented for a high power microwave/millimeter wave amplifier (herein called CEBA) that requires no radio frequency (RF) circuit structure. The electron beam is treated as an active dielectric serving the dual purpose of slow-wave circuit and amplification source. Amplification is obtained when beam-wave synchronism is met.

The RF wave, generated by an antenna, propagates inside an oversized wave-

DD FORM 1 JAN 73 1473 EDITION OF 1 NOV 65 IS OBSOLETE

UNCLASSIFIED

SECURITY CLASSIFICATION OF THIS PAGE (When Data Entered)

420698

#20 - ABSTRACT (Contd.)

guide and interacts with a solid or hollow electron beam that guides the RF energy. Two theories are presented for achieving an electron beam with isotropic permittivity and permeability characteristics. The electron beam and magnetic field parameters for obtaining this isotropic condition are given and the importance of the cyclotron frequency and Doppler effect are described for achieving low voltage and low magnetic field operation. The RF field that can propagate on the electron beam is characterized by the electric field equal to the magnetic field multiplied by the intrinsic impedance and the imaginary j phase factor. The boundary value problem is solved with emphasis on solutions for the lowest order mode. Computer generated design data show the propagation constant and growth factor as functions of frequency for selected values of plasma and cyclotron frequencies; bandwidth characteristics; and beam parameters. Experimental data is given that correlates with the computer data and gives support to the concept that the electron beam as an active dielectirc medium can serve the dual purpose of slow-wave circuit and amplication source.

The important features of low voltage, low magnetic field, and low cost make the CEBA attractive for use as a lightweight inexpensive millimeter wave amplifier for airborne and tactical applications. These attractive features are indicative of potential advantages over relativistic interaction devices such as the gyrotron which requires very high voltages and super-conducting solenoids, and slow-wave interaction devices such as the coupled cavity traveling-wave tube which requires very expensive RF circuit structures at millimeter frequencies.

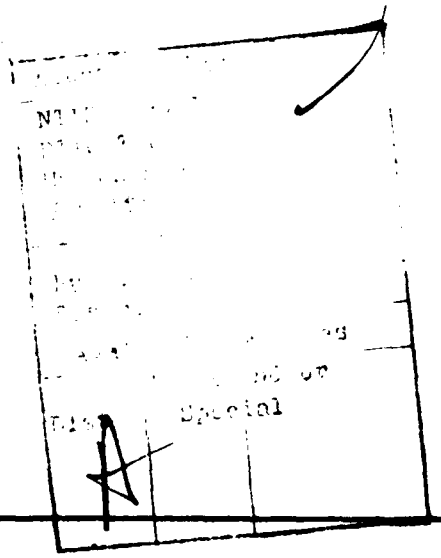

CONTENTS

FIGURES

CONTENTS (CONTD)

TABLE

CIRCUITLESS ELECTRON BEAM AMPLIFIER (CEBA)

BACKGROUND

An In-House Laboratory Independent Research (ILIR) program was initiated in October 1979 to demonstrate feasibility of a high power millimeter (mm) wave amplifier that will not require a radio frequency (RF) circuit. The program is being conducted in three separate phases (each one year duration).

During phase I, the generation, propagation and growth of RF energy on electron beams in the microwave and mm wave regions were investigated. Emphasis was placed on high perveance electron beams. Theoretical results characterized the dielectric properties of the electron beam and a theory was developed describing circuitless RF wave-electron beam interaction. Preliminary experiments were performed to examine certain characteristics of the theory such as dependence on magnetic field and operating voltage with wave growth.

The phase II effort is to experimentally demonstrate that the velocity of RF energy can be decreased when traveling in direct proximity to a high current electron beam. Work under phase II will include modification of the apparatus built under phase I to include an electron gun and collector; magnetic field structure; RF velocity timing circuit; and parts and subassemblies needed to obtain a high vacuum (less than 10^{-6} torr). Correlation between theory and experiment will be obtained by examining the interaction of the RF energy with the electron beam for different current densities and magnetic fields.

In phase III, the feasibility of a Ku-Band device operating in a pulsed, low-duty mode will be demonstrated. The experimental apparatus used in phases I and II will be modified so that a higher current density beam (greater than 100 amperes per square centimeter) can be generated in order to obtain low voltage operation, synchronism, and interaction between beam and RF energy. The design parameters of the device will be optimized and design changes implemented from the data obtained from both phases I and II.

This report covers work done under phase I of the program from October 1979 through September 1980.

INTRODUCTION

The impetus for this study is the need for RF power in the mm and near mm wave regimes for airborne and tactical applications. Transmitter packages are urgently needed for surveillance, fire control, and air defense radars capable of operating in smoke, fog, and inclement weather. For these applications, low voltage, simple construction, lightweight, low cost, and high efficiency are desirable features. Currently there are several types of devices providing RF power in the mm wave regime: solid-state diodes have demonstrated several watts of RF power under pulsed, low duty conditions at 95 gigahertz (GHz); extended interaction oscillators (EIOs) have produced about 1 kilowatt (kW) peak RF at low duty cycles; and traveling-wave tubes (TWTs) have produced about 1 kW of peak RF power at

medium duty cycles at 95 GHz.

If higher powers and longer duty cycles are to be achieved by solid-state devices, they must be made to be extremely efficient in order to compete with electron beam vacuum devices. Heat dissipation could be an insurmountable problem since a solid-state device, by its operating nature, must occupy a small physical area. Vacuum devices (tubes) can also benefit from increased efficiency, but a major consideration with tubes at mm wave frequencies is cost. The high cost of tubes is mainly due to high vacuum operation, high precision manufacturing requirements, and the complexity of the tube, in particular the RF circuit structure. Note that a tube producing 10 watts of RF power at mm wave frequencies can be as complex as a 1 kW version. Another high cost factor is that tubes tend to operate at high voltages (10 kilovolts - 80 kilovolts (kV)) unlike solid-state devices that operate at low voltages (5- 30 volts). Thus the high voltage supply and ancillary equipment needed to operate the tube not only increase the subsystem weight but also add a significant amount to the total cost. Vacuum devices are expected to be the only source of high power in the mm wave region for the foreseeable future, so that device simplicity and cost reduction are very important design considerations.

As was mentioned above, a very costly item in mm wave tubes is the RF wave circuit structure. In some cases the RF circuits represent as much as 60 percent of the total cost of a tube. Over past years, attempts have been made to build microwave oscillators and amplifiers which did not require an RF slow wave circuit, i.e., such devices as the scalloping beam amplifier,[1] the double stream amplifier,[2] and the resistive wall amplifier.[3] These devices were abandoned because the conventional devices such as the klystron, magnetron, and TWT demonstrated superior performance characteristics. Perhaps, however, it is time to reconsider the circuitless devices for mm wave operation because of their inherent simplicity.

Devices based upon relativistic mechanisms have received great attention in recent years. One such device is the gyrotron. The Russians, utilizing relativistic interactions, have obtained impressive RF output power (30 kW pulsed) with greater than 40 percent efficiency at 35 GHz and hundreds of kW of peak RF power at an efficiency of 15 percent.[4] Of course, at the present state-of-the-art, the gyrotron requires very high magnetic fields and beam voltages, and still has not left the laboratory (at least in the United States).

---

1 T. G. Mihran, "Scalloped Beam Amplification," IRE Transactions - Electron Devices, ED-3, p. 32, Jan 1956.

2 J. R. Pierce, W. B. Hebenstreit, "A New Type of High Frequency Amplifier," Bell System Technical Journal, Vol. 28, pp. 33-51, Jan 1949.

3 C. K. Birdsall, G. R. Brewer, A. V. Haeff, "Resistive Wall Amplifier," Proc. IRE, Vol. 41, p. 865, 1953.

4 J. M. Baird, "Survey of Fast Wave Tube Developments," IEDM Technical Digest, p. 159, 1979.

This report details the study of a novel Circuitless Electron Beam Amplifier, herein called CEBA, which does not require an RF circuit structure but is based upon a slow-wave interaction mechanism. The electron beam is treated as an active dielectric waveguide serving the dual purpose of slow-wave circuit and amplication source. The CEBA uses a dense electron beam whose effective dielectric constant ϵ_r, can be increased to a high value (ϵ_r greater than 10). The RF energy launched by an antenna, propagates inside an oversized waveguide and interacts with the high density hollow or solid electron beam that guides and amplifies the RF energy. Furthermore, only a modest amount of magnetic field is required, and the accelerating voltage can be made low since the dielectric constant of the electron beam "waveguide" causes a reduction in the phase velocity of the RF wave which is propagating along the electron beam. Low magnetic field, low voltage, and the potential for low cost make the CEBA attractive for use as a lightweight inexpensive mm wave amplifier for airborne and tactical applications. These features are indicative of potential advantages over relativistic interaction mechanism devices such as the gyrotron which requires very high voltages and super-conductive solenoids, and slow-wave interaction mechanism devices such as the coupled-cavity TWT which requires very expensive RF circuit structures at mm wave frequencies.

In the following sections, a detailed description of the CEBA is presented including the theory of operation; computer and experimental data obtained to-date; important conclusions; and future plans concerning work on the CEBA and, in particular, additional tasks to be completed under phase II of the ILIR program.

DESCRIPTION OF THE CEBA

Figure 1 is a cross-sectional, schematic view of the CEBA. The RF input and output are directive, circularly polarized antennas located outside the vacuum housing. Helical antennas could also be used inside the vacuum housing to generate circularly polarized radiation, however, affixing the antennas in relationship to the electron beam could complicate the construction of the device. The magnetic field, collector and power sources are conventional components. The cathode is a thermionic emitter configured to produce a hollow high current density beam. The RF energy propagating along the z axis encounters a region of gradually increasing charge density. As can be seen from Figure 1, the CEBA has no RF circuit and can be a device of simple construction.

In the following section a theoretical analysis is presented that describes circuitless RF wave-electron beam interaction in an electron beam characterized as a high dielectric constant medium. Two methods are given for obtaining an electron beam with an isotropic permittivity ϵ, and/or permeability μ. One method utilizes transverse and longitudinal direct current (dc) magnetic fields and the second method utilizes only a longitudinal dc magnetic field. For the first method a transverse magnetic field component can be obtained by incorporating in the CEBA an axial current carrying wire (not shown in Figure 1).

THEORETICAL ANALYSIS

In adopting a model for a plasma, one can use a dielectric model or a

conducting model. The relative dielectric constant ϵ_r, and the conductivity σ, of a plasma are related by the following expression[5]

$$\epsilon_r = 1 + \frac{j\sigma}{\omega \epsilon_0} \tag{1}$$

where ϵ_0 is the dielectric constant in a vacuum and $\epsilon_0 \epsilon_r = \epsilon$. The choice of models used for an isotropic plasma is one of convenience depending on the particular problem considered. The authors chose the dielectric model. In certain situations, such as the ionosphere or a tenuous plasma, the relative dielectric constant for transverse electromagnetic (EM) waves is given by:

$$\epsilon_r = 1 - \frac{\omega_p^2}{\omega^2} \tag{2}$$

where ω is the operating frequency, ω_p is the plasma frequency $= \sqrt{\frac{\rho \eta_e}{\epsilon_0}}$, ρ is the charge density and η_e is the charge to mass ratio $\frac{e}{m}$.

J. Blewett and S. Ramo[6] investigated theoretically and experimentally the transmission of EM waves of the symmetrical, transverse magnetic type by a space charge of uniform density, rotating under the influence of a uniform magnetic field. They found by appropriate adjustments of magnetic field, the dielectric constant as given by Equation (2) above, can be reduced to zero and even made negative. The experiments showed that the propagation constant of the EM wave could be controlled by varying the dielectric constant of the rotating space charge medium.

When the plasma is drifting and is confined in a static magnetic field, Equation (2) becomes

$$\epsilon_r = 1 - \frac{(\omega_p/\omega)^2}{1 \pm \omega_c/\omega} \tag{3}$$

as shown in Appendices A and B. Also ω_c is the cyclotron frequency $= \eta_e B_0$ and B_0 is the magnetic field intensity. In general, the dielectric constant of the plasma in a longitudinal magnetic field is not isotropic, and ϵ_r in all transverse directions is given by Equation (3) and is given by Equation (2) in the propagation direction. However, under specialized conditions, the authors were able to characterize an electron beam as having an isotropic permittivity ϵ, and permeability μ where ϵ_r and μ_r are both given by Equation (3). In addition, the electron beam is defined by electric and magnetic current desnities $\vec{J}$ and $\vec{M}$ respectively in all three directions (r, φ , z) of the orthogonal coordinate system.

Appendix A gives the derivation of an electron beam with an isotropic permittivity ϵ, and/or permeability μ in transverse and longitudinal dc magnetic fields. A condition of the derivation requires a dc magnetic field

---

5 E. H. Holt, R. E. Haskell, "Foundations of Plasma Dynamics," Mac Millan Co., N.Y., p. 197, 1968.

6 J. Blewett, S. Ramo, "Propagation of Electromagnetic Waves in a Space Charge Rotating in a Magnetic Field," Journal of Applied Physics, Vol. 12 pp. 856-859, 1941.

in at least two directions (r and z or φ and z). A practical method is to generate a B_φ magnetic field by using an axial longitudinal current carrying wire.

Appendix B gives the derivation of an electron beam with an isotropic permittivity ϵ, and/or permeability μ in only a longitudinal magnetic field. A condition of this derivation requires that

$$\kappa u_o = \pm \omega_c \tag{4}$$

where κ is the longitudinal propagation constant and u_o is the average electron velocity.

The principal of operation for the CEBA is based upon the premise that the relative dielectric constant ϵ_r (and the relative permeability μ_r) of an electron beam for propagating waves having nearly circular polarization can be varied by adjusting the charge density of the beam and the applied magnetic field. In examining Equation (3)

$$\epsilon_r = \mu_r = 1 - \frac{(\omega_p/\omega)^2}{1 \pm \omega_c/\omega} \tag{5}$$

if one choose the negative sign (representing a given polarization sense) in the denominator and $\omega \to \omega_c$ then ϵ_r, $\mu_r \to +\infty$, independent of the value of the charge density. However, for high current densities ($J_o > 100$ A/cm^2) large values of ϵ_r and μ_r can be achieved when ω deviates from ω_c.

Figure 2 shows the variation of ϵ_r with frequency for a cyclotron frequency, $\omega_c = 50 \cdot 10^9 \frac{\text{rad}}{\text{sec}}$ and various plasma frequencies, ω_p. Note that ϵ_r increases to large values with increasing plasma frequency or as the operating frequency approaches the cyclotron frequency. For positive ϵ_r, $\omega_c \gtrsim \omega$. For the chosen cyclotron frequency, a magnetic field $B_{cyc} = 2800$ gauss is required. The table of values given in Figure 2 shows the equivalent current densities and Brilloin focusing fields. Since 2800 gauss is required in this example, the plasma frequency cannot exceed about $30 \cdot 10^9 \frac{\text{rad}}{\text{sec}}$ for a practical realization.

An RF plane wave propagating in this beam would have a phase velocity given by:

$$v_p = \frac{c}{\sqrt{\epsilon_r \mu_r}} = \frac{c}{\epsilon_r} \tag{6}$$

where C, is the velocity of light in a vacuum. For large values of ϵ_r and/or μ_r the phase velocity can be significantly small compared to the velocity of light. When electrons of the medium are caused to drift at a velocity near the phase velocity of the RF wave, then interaction between beam and wave is achieved and gain in the traveling-wave tube sense should be expected. The electron beam, in effect, guides and slows the RF wave just as in a dielectric waveguide, and no RF circuit is needed. It should be mentioned here that computer data (see Computer Data section) shows that the

phase velocity of the RF wave is not necessarily identical to the phase velocity of the plane wave as given by Equation (6). For the cases examined, the phase velocity of the plane wave is somewhat slower than the phase velocity of the RF wave propagating through the electron beam.

The general system studied consists of two regions. The first region is a solid electron beam in an axial magnetic field which has both electric and magnetic current densities $\vec{J}$ and $\vec{M}$ such that

$$\vec{M} = \pm j\eta\vec{J} \quad \text{or} \quad \vec{M} = \pm j\sqrt{\mu/\epsilon}\,\vec{J} \tag{7}$$

Equation (7) is based upon the notion that the helical path of an electron or group of electrons in an axial magnetic field can be resolved as:

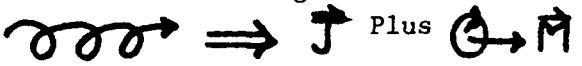

The second region is free space surrounding the electron beam.

The solution to the problem consists of two parts; the high current density electron beam and the EM energy propagating through this beam (as described by the electric and magnetic current densities given above). The first part of the problem has essentially been solved and is given by Equation (5) rewritten as:

$$\frac{\beta}{\beta_0} = 1 - \frac{(\omega_p/\omega)^2}{1 - \omega_c/\omega} \tag{8}$$

where $\beta_0 = \omega\sqrt{\epsilon_0/\mu_0}$ is the free space propagation constant and $\beta = \omega\sqrt{\epsilon/\mu}$ is the propagation constant of a plane wave in the dielectric medium (electron beam). The relationship that $\kappa\mu_0 \simeq \omega_c$ is assumed to exist. This is consistent with the derviation for an isotropic ϵ_r as given in Appendix B. The second part of the problem is a boundary value problem and one must first determine the EM field expressions by solving Maxwell's equations. A relationship similar to Equation (7) is assumed to exist between the electric and magnetic fields.[7] The relationship is given by

$$\vec{E} = \pm j\eta\vec{H} \text{ (beam region) and } \vec{E} = \pm j\eta_0\vec{H} \text{ (free space)} \tag{9}$$

where $\eta = \sqrt{\mu/\epsilon}$ and $\eta_0 = \sqrt{\mu_0/\epsilon_0}$. In order to obtain a positive β/β_0 (forward wave), one must choose different signs in the two regions for Equations (9). For $\vec{E} = -j\eta\vec{H}$ and $\vec{E} = +j\eta_0\vec{H}$, β/β_0 is positive. Appendix C gives the derivation for the field expressions in the two regions. The fields have the form

$$E, H \propto A(r,\varphi)\exp\left[j(\omega t - \gamma_z z + N\varphi)\right] \tag{10}$$

where γ_z is complex and is the propagation constant in the z direction, and

---

7 V. H. Rumsey, "A New Way of Solving Maxwell's Equations," IRE Transactions on Antennas and Propagation, pp. 461-465, Sep 1961.

$$A(r,\varphi)=\begin{cases} J_N(\gamma_r r) \text{ or } I_N(\gamma_r r) & \text{For } r \le r_o \\ K_N(\gamma_r r) & r \ge r_o \end{cases} \quad (11)$$

γ_r and K_o are complex radial propagation constants and r_o is the beam radius. The $I_N(\gamma_r r)$ function was used to characterize the fields in the beam region since it is consistent with the isotoric $\epsilon_r(\mu_r)$ (See Appendix C). The authors have, presently, limited the investigation to the $N=0$ modes. When $N \neq 0$, a nearly circularly polarized mode in the electron beam region exists.

The derivation of the characteristic (root) equation is given in Appendix C, and is

$$\frac{\beta}{\gamma_r}\frac{I_1(\gamma_r r_o)}{I_0(\gamma_r r_o)} = \frac{\beta_o}{K_o}\frac{K_1(K_o r_o)}{K_0(K_o r_o)} \quad (12)$$

The above equation involves Bessel functions with complex arguments and can be separated into the real and imaginary parts to give

$$\frac{\beta_o}{\beta} = Re\left[\frac{K_o}{\gamma_r}\frac{I_1(\gamma_r r_o)}{I_0(\gamma_r r_o)}\frac{K_0(K_o r_o)}{K_1(K_o r_o)}\right] \quad (13)$$

and

$$0 = Im\left[\frac{K_o}{\gamma_r}\frac{I_1(\gamma_r r_o)}{I_0(\gamma_r r_o)}\frac{K_0(K_o r_o)}{K_1(K_o r_o)}\right] \quad (14)$$

where $\gamma_r r_o = \rho e^{j\varphi}$ and $K_o r_o = \xi e^{j\theta}$

The method of obtaining Equations (13) and (14) in explicit forms from Equation (12) is given in Appendix C along with the definitions of the terms used. What is important is that complex roots have been found which give forward wave propagation and gain.

The next section gives computer data obtained by utilizing the beam Equation (8) and characteristic Equations (13) and (14).

COMPUTER DATA

A Hewlett Packard 9820A desk top calculator and the 9862A calculator plotter were utilized to obtain the data.

The approach taken was to first select three of the four quantities, $\xi, \theta, \rho, \varphi$ and then search for the fourth to satisfy the root Equation (14). The $J_0(\rho e^{j\varphi})$ and $J_1(\rho e^{j\varphi})$ functions were programmed into the computer as series expansions.[8] Due to the complexity of the series expansions for Y_N,

8 Table of the Bessel Functions $J_0(z)$ and $J_1(z)$ For Complex Arguments, National Bureau of Standards, Second Edition, pp. vii-381, Jan 1947.

needed to find the K_N, they were not programmed into the computer. Instead, tabulated values were used.[9] Values are tabulated for $\xi = 0$ in steps of 0.01 to $\xi = 10$ and for $\theta = 0^\circ$ to 90° in steps of 5°. This necessitated the selection of both ξ and θ. Thus we chose to select ξ, θ, ρ and search for φ.

The ranges of $\xi, \theta, \rho, \varphi$ become restricted because of the propagation constant equations $\gamma_r^2 = \gamma_z^2 - \beta^2$ and $K_0^2 = \gamma_z^2 - \beta_0^2$. One can expand the γ_r^2 equation into real and imaginary parts since $\gamma_r = \frac{\rho}{r_0} e^{j\varphi}$ and $\gamma_z = \alpha + j\alpha$

This expansion gives

$$\text{Real:} \quad \left(\frac{\rho}{r_0}\right)^2 \cos(2\varphi) = \alpha^2 - \alpha^2 - \beta^2 \tag{15}$$

and

$$\text{Imag:} \quad \left(\frac{\rho}{r_0}\right)^2 \sin(2\varphi) = 2\alpha\alpha \tag{16}$$

Likewise, the K_0^2 equation is expanded into real and imaginary parts since $K_0 = \frac{\xi}{r_0} e^{j\theta}$. This expansion gives Real: $\left(\frac{\xi}{r_0}\right)^2 \cos(2\theta) = \alpha^2 - \alpha^2 - \beta_0^2$ (17)

and Imag:

$$\left(\frac{\xi}{r_0}\right)^2 \sin(2\theta) = 2\alpha\alpha \tag{18}$$

Substracting Equation (15) from Equation (17) and equating Equations (16) and (18) yields

$$\xi^2 \cos(2\theta) - \rho^2 \cos(2\varphi) = (\beta^2 - \beta_0^2) r_0^2 = N^2 \tag{19}$$

and

$$\rho^2 \sin(2\varphi) = \xi^2 \sin(2\theta) \tag{20}$$

Equation (20) restricts the range of the four quantities $\xi, \theta, \rho, \varphi$. Having found a root by using Equations (14) and (20), then Equations (13) and (19) are used to find the frequency associated with that root.

In summary, given $\xi, \theta, \rho, \varphi$ satisfying Equations (14) and (20), Equation (13) returns $M \triangleq \frac{\beta_0}{\beta}$ and Equation (19) returns $N^2 \triangleq (\beta^2 - \beta_0^2) r_0^2$

thus $N^2 = \beta^2 r_0^2 \left(1 - \frac{\beta_0^2}{\beta^2}\right) = \beta^2 r_0^2 \left(1 - M^2\right)$ and $\beta_0 = M\beta$

therefore,

$$\beta_0 = \frac{MN}{r_0 \sqrt{1 - M^2}} . \tag{21}$$

---

9 Table of the Bessel Functions $Y_0(z)$ and $Y_1(z)$ For Complex Arguments, National Bureau of Standards, pp. vii-402, Jan 1949.

The values for κ and α are determined from either Equations (15) and (16) or Equations (17) and (18) therefore,

$$\kappa = \pm \left[\frac{(\beta^2 + \rho^2/r_o^2 \cos(2\varphi)) \pm \sqrt{\beta^4 + \rho^4/r_o^4 + 2\beta^2\rho^2/r_o^2 \cos(2\varphi)}}{2} \right]^{\frac{1}{2}} \quad (22)$$

and

$$\alpha = \frac{\rho^2 \sin(2\varphi)}{2 r_o^2 \kappa} \quad (23)$$

Many more roots were found then apply to the particular approximations made in the theory. The roots must satisfy approximately the condition that $\beta \simeq \kappa \gg \alpha$. The reason is that Equation (5) for $\epsilon_r(\mu_r)$ was derived ignoring the growth term α. This implies that $\kappa \gg \alpha$. In the derivation given in Appendix B $v_1 \simeq v_2$ which implies $\kappa \simeq \beta$. Fast wave solutions were found for which

$$0.3 \leq \frac{\beta_o}{\beta} \leq 1.0$$

and these roots satisfy the above approximations. These fast waves are of interest but in this report the authors are most interested in slow wave solutions because of low voltage operation. The reason for this is, the capability exists in-house to conduct experiments for the purpose of demonstrating beam-wave interaction.

Slow wave solutions were found in the range of $\theta = 20^o$ to 70^o. Since θ could only be selected in steps of 5^o, the 20^o and 70^o limits only approximate the passband limits. No slow wave solutions were found from $\theta = 0^o$ to 15^o and $\theta = 75^o$ to 90^o. Figure 3 is an ω vs. β plot. The passband limits approach a vertex between $\beta = 12.0$ rad/cm and $\beta = 13.0$ rad/cm. In the region defined by the $\theta = 20^o$ and 70^o rays, an infinite number of roots exist. However, Equation (8) (beam equation) must still be considered. The intersection of the curves defined by both the beam equation and characteristic equation will give the ω-β plot useful for characterizing the CEBA. Figures 4 and 5 are the ω-κ plot and ω-α plot respectively. These plots also, only display the roots of the characteristic equation. Note that the ω-κ plot is of most interest since κ is the axial propagation constant of the wave on the beam. Table 1 gives tabulated data for the 20^o, 45^o, and 70^o rays. One can see from Table 1 that ϵ_r varies over a wide range from 2 to 65 and decreases with increasing frequency. Also, notice that α in most cases is smaller than κ and β. The data given in Table 1 is for $r_o = 3$ mm which is a large diameter beam. The frequency varies inversely with r_o (Equation (21)), therefore, slow wave interaction at mm wavelengths is possible for r_o about 1 mm.

Figures 6, 7, and 8 are ω-β, ω-κ, and ω-α plots for the CEBA which are indicative of the device characteristics and include the curves generated from the beam Equation (8) and characteristic Equation (14). The plots are for fixed values of $r_o = 3$ mm, $\omega_c = 50 \times 10^9$ rad/sec, and $\omega_p = 10$, 20, 30, 40, and 50×10^9 rad/sec. Figure 7 shows that the

$\frac{v}{c}$ = 0.2 (10 kV) intersects the ω-β curve for $\omega \simeq 23 \times 10^9$ rad/sec. In Figure 8 note that for $\omega_p = 40 \times 10^9$ rad/sec and α = 12.0 dB/cm implies a growth factor greater than 60 decibels (dB) for a 2 inch interaction region.

EXPERIMENTAL DATA

Experiments were conducted in order to verify some aspects of the theory . A transverse wave TWT(TWTWT) was used which was developed some years ago under an Army program.[10] The TWTWT has a twisted two-wire transmission line circuit (a bi-filar helix with a large pitch) and utilizes a cylindrical electron beam in an axial magnetic field. The TWTWT is transparent (no internal attenuation) and can be operated in a "push-pull" arrangement to produce a circularly polarized wave. Figure 9 is a picture of the TWTWT and associated test equipment.

Interaction was observed and measured over a small range of frequencies. A given input RF signal produced an increase in output signal as opposed to oscillations which were also observed. The TWTWT had poor RF matches and no attenuator which contributed to oscillations. The measured results are shown in Figure 10. The curves of Figure 10 show a break around the "average" cyclotron frequency and the curves have slightly different slopes. Note that the theoretical dielectric beam Equation (9) has a pole when $\omega = \omega_c$ indicative of the measured result. A difference was observed when the magnetic field direction was reversed, in that the beam voltage and magnetic field settings were more critical for maintaining synchronism between beam and wave. This observation is also consistent with the theory except that a stronger effect was expected. A space charge wave interaction has been ruled out since one would expect a much higher beam voltage than was needed for interaction and because of the magnetic field dependence. The cyclotron wave interaction is not completely ruled out but is unlikely because of the reasons given below. The TWTWT was originally designed for the slow cyclotron wave interaction. The original design parameters of the TWTWT for the cyclotron wave interaction are:

$\omega_c = 15.3 \times 10^9$ rad/cm, $\omega = 22.7 \times 10^9$ rad/cm, $\frac{\omega_c}{\omega} = 0.674$,

and beam voltage = 1725 volts. The curves in Figure 10 are for ω_c/ω varying from 0.8 to 1.2 which is larger than the design value. Also, the voltage is less than half of the design voltage of 1725 volts. Interaction of a circuit wave with the slow cyclotron wave on the beam should occur for a "filamentary" beam approximation[11] according to the diagram shown in Figure 11. Interaction can occur over a wide range of frequencies, depending upon the operating voltage. Note, however, that there is no break in the curve near ω_c and that the slope is constant. This does not agree with the experimental measurements obtained in the TWTWT.

10 S. F. Paik, "Study of Cyclotron and Synchronous Wave Devices," ECOM-0398-4 Technical Report, DAAB07-68-C-0398, July 1970.

11 A. H. Gottfried, "Theory and Design of Cyclotron-Wave Traveling-Wave Amplifiers," Doctorate Thesis, New Jersey Institute of Technology, Newark, N.J., 1979.

The theory presented in this paper predicts a break in the curve at the cyclotron frequency and a difference in operating mode above and below the cyclotron frequency.

As a final observation, the experimental curves of Figure 10 agree qualitatively with the theoretical results as shown in Figure 7. A quantitative comparison can not be made since the exact radius of the beam for the TWTWT is unknown and it also had an RF circuit.

DOPPLER EFFECT

This discussion on the Doppler effect is included because there is a possibility that the magnetic field requirement will be drastically reduced due to the Doppler effect in the dense electron beam. Consider the following:

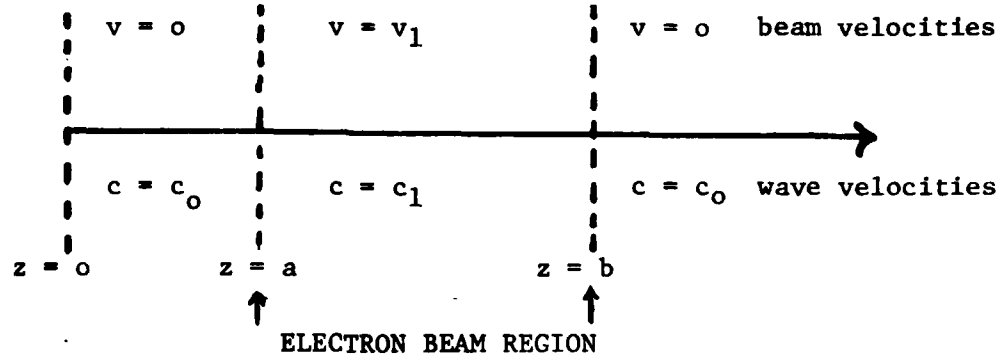

For $0 \leq z < a$, the transverse field components (in Cartesian coordinates) are:

$$E_x = Ae^{j\omega_0(t - z/c_0)}$$

$$E_y = jAe^{j\omega_0(t - z/c_0)}$$

For $a \leq z \leq b$

$$E_x = Be^{j\omega_0(t - z/c_1)}$$

$$E_y = jBe^{j\omega_0(t - z/c_1)}$$

Laboratory coordinates

$$E_x = B'e^{j\omega_0\left(t - \frac{z'}{c_1 - v_1}\right)}$$

$$E_y = jB'e^{j\omega_0\left(t - \frac{z'}{c_1 - v_1}\right)}$$

in coordinate system moving with the beam at velocity V_1

where $\omega_D = \omega_0(1 - V_1/c_1)$ represents the Doppler frequency. The frequency "seen" by the electrons should be affected by the relative velocity between the electrons and the wave propagating in the beam.

For $b \leq z$

$$E_x = C e^{j\omega_0(t - z/c_0)}$$

$$E_y = jC e^{j\omega_0(t - z/c_0)}$$

Postulate that in the beam region for $a \leq z \leq b$, Equation (5) can be written as

$$\epsilon_r = 1 - \frac{(\omega_p/\omega_D)^2}{1 - \omega_c/\omega_D} \tag{24}$$

As an example, consider the difference in the velocity of the wave and the electron beam $(c_1 - V_1) \simeq 0.1 c_0$, $V_1 \simeq 0.1 c_0$, and $\omega_D \simeq \omega_c$. Then $c_1 \simeq 0.2 c_0$

and $$\omega_0 = \frac{\omega_D}{1 - V_1/c_1} \simeq \frac{\omega_c c_1}{c_1 - V_1} \simeq 2\omega_c \tag{25}$$

The above example shows that for a given operating frequency ω_0, the cyclotron frequency is reduced by half. As $c_1 \rightarrow V_1$, even more drastic reductions are possible. However, there is a physical limit to the reduction imposed by the magnetic focussing requirements.

CONCLUSIONS

A theory has been formulated that describes the principles of operation for a CEBA. Two methods were presented for achieving an isotropic $\epsilon_r(\omega_p)$. Assumptions and approximations were made and the boundary value problem was solved for EM waves propagating through an electron beam considered as a dielectric medium. Slow and fast wave solutions were found which are consistent with the theory. Tabulated data and plots are given which show dispersion characteristics and wave growth for fixed values of the plasma and cyclotron frequencies. Experiments were performed on a TWTWT which lend credibility to the theory and qualitative correlation with the computer data. A brief discussion on the Doppler effect was included to give the reader an insight into the possibility of the CEBA operating with a drastically reduced magnetic field.

The desirable features of no RF circuit, low voltage operation, low magnetic field, and potential low cost make the CEBA attractive for use as a lightweight inexpensive mm wave amplifier for airborne and tactical applications.

FUTURE PLANS

This report covers work done under an ILIR program from October 1979 to October 1980. A Follow-on (Phase II) ILIR program has been initiated

and will continue through FY-81. A purpose of the Phase II effort is to demonstrate that the velocity of RF energy can be decreased when traveling in direct proximity to a high current density electron beam. A demountable, circuitless device similar to the CEBA shown in Figure 1 will be built and tested. Experiments will be performed in an effort to obtain correlation with the theory presented in this paper and in addition to observe and measure beam-wave interaction. The theory as presented requires an isotropic ϵ_p and μ_p. Plans are to extend the theory to include an ϵ_p characterized by a diagonal matrix as given below:

$$\epsilon_r(\mu_r) = \begin{pmatrix} 1 - \dfrac{(\omega_p/\omega)^2}{1 - \frac{\beta k v_0}{\omega} \pm \frac{\omega_c}{\omega}} & 0 & 0 \\ 0 & 1 - \dfrac{(\omega_p/\omega)^2}{1 - \frac{\beta k v_0}{\omega} \pm \frac{\omega_c}{\omega}} & 0 \\ 0 & 0 & 1 - \dfrac{(\omega_p/\omega)^2}{1 - \frac{\beta k v_0}{\omega}} \end{pmatrix} \quad (26)$$

Equation 26 has been recently derived by the authors as part of a more general dielectric beam theory in which some of the approximations of the theory presented in this report are eliminated. This work will be reported on in the remaining phases of the program. Maxwell's equations are still separable when ϵ_p has the above form but determination of the roots of the characteristic equation is more complicated. The authors feel that this analysis is necessary because the conditions imposed on the theory are less restrictive and also because it opens the possibility for other modes of operation which could have more favorable characteristics.

ACKNOWLEDGMENT

The authors are especially grateful to Dr. F. Schwering, CORADCOM, Fort Monmouth, NJ for collaboration in writing the section on the Doppler effect.

REFERENCES

1. T. G. Mihran, "Scalloped Beam Amplification," IRE Transactions - Electron Devices, ED-3, p. 32, Jan 1956.

2. J. R. Pierce, W. B. Hebenstreit, "A New Type of High Frequency Amplifier," Bell System Technical Journal, Vol. 28, pp. 33-51, Jan 1949.

3. C. K. Birdsall, G. R. Brewer, A. V. Haeff, "Resistive Wall Amplifier," Proc. IRE, Vol. 41, p. 865, 1953.

4. J. M. Baird, "Survey of Fast Wave Tube Developments," IEDM Technical Digest, p. 159, 1979.

5. E. H. Holt, R. E. Haskell, "Foundations of Plasma Dynamics," Mac Millan Co., N.Y., p. 197, 1968.

6. J. Blewett, S. Ramo, "Propagation of Electromagnetic Waves in a Space Charge Rotating in a Magnetic Field," Journal of Applied Physics, Vol. 12, pp. 856-859, 1941.

7. V. H. Rumsey, "A New Way of Solving Maxwell's Equations," IRE Transactions on Antennas and Propagation, pp. 461-465, Sep 1961.

8. Table of the Bessel Functions $J_0(z)$ and $J_1(z)$ For Complex Arguments, National Bureau of Standards, Second Edition, pp. vii-381, Jan 1947.

9. Table of the Bessel Functions $Y_0(z)$ and $Y_1(z)$ For Complex Arguments, National Bureau of Standards, pp. vii-402, Jan 1949.

10. S. F. Paik, "Study of Cyclotron and Synchronous Wave Devices," ECOM-0398-4 Technical Report, DAAB07-68-C-0398, July 1970.

11. A. H. Gottfried, "Theory and Design of Cyclotron-Wave Traveling-Wave Amplifiers," Doctorate Thesis, New Jersey Institute of Technology, Newark, N.J., 1979.

12. J. D. Jackson, "Classical Electrodynamics," John Wiley & Sons, Inc., p. 228, 1962.

13. Handbook of Mathematical Functions with Formulas, Graphs, and Mathematical Tables," US Department of Commerce, NBS, pp. 355-436, June 1964.

14. Table of Bessel Functions - Op Cit #8

15. Table of Bessel Functions - Op Cit #9

16. Handbook of Mathematical Functions - Op Cit #13

17. Table of Bessel Functions - Op Cit #9

GLOSSARY OF SYMBOLS

B_0	dc magnetic induction in z direction
B_φ	dc magnetic induction in φ direction
c	velocity of light in free space
$\vec{E}$	ac electric field intensity
$\vec{H}$	ac magnetic field intensity
I_N	modified Bessel function of the first kind
J_N	Bessel function of the first kind
$\vec{J}$	electric current density
K_N	modified Bessel function of the second kind
K_0	complex radial propagation constant equal to $\sqrt{\gamma_z^2 - \beta_0^2}$
$\vec{M}$	magnetic current density
N	order of Bessel function is a positive or negative integer
r_0	radius of electron beam
U_0	average electron drift velocity
V_p	phase velocity of RF wave
Y_N	Bessel function of the second kind
α	wave growth factor
β	propagation constant of plane wave in the beam and equals $\omega\sqrt{\mu\epsilon}$
β_0	propagation constant of plane wave in free space and equals $\omega\sqrt{\mu_0 \epsilon_0}$
γ_r	radial complex propagation constant and equals $\sqrt{\gamma_z^2 - \beta^2}$
γ_z	longitudinal complex propagation constant and equals $\alpha + j\alpha$
ϵ	permittivity in the electron beam region
ϵ_0	permittivity in free space

ϵ_r effective relative permittivity

η impedance in beam region and equals $\sqrt{\mu/\epsilon}$ ohms

η_o impedance in free space and equals $\sqrt{\mu_o/\epsilon_o}$ ohms

η_e charge to mass ratio

θ phase angle of $K_o r_o$

k longitudinal propagation constant

μ permeability in the electron beam region

μ_o permeability in free space

μ_r effective relative permeability

ξ amplitude of $K_o r_o$

ρ amplitude of $\gamma_r r_o$

ρ_o charge density

σ conductivity, where

$$\sigma = j\omega\epsilon_o(1-\epsilon_r)$$

τ $\psi + \pi/2$

ϕ $\theta + \pi/2$

χ_E electric susceptibility

χ_M magnetic susceptibility

ψ phase angle of $\gamma_r r_o$

ω operating frequency in radians/second

ω_c cyclotron frequency in radians/second

ω_D Doppler frequency in radians/second

ω_p plasma frequency in radians/second

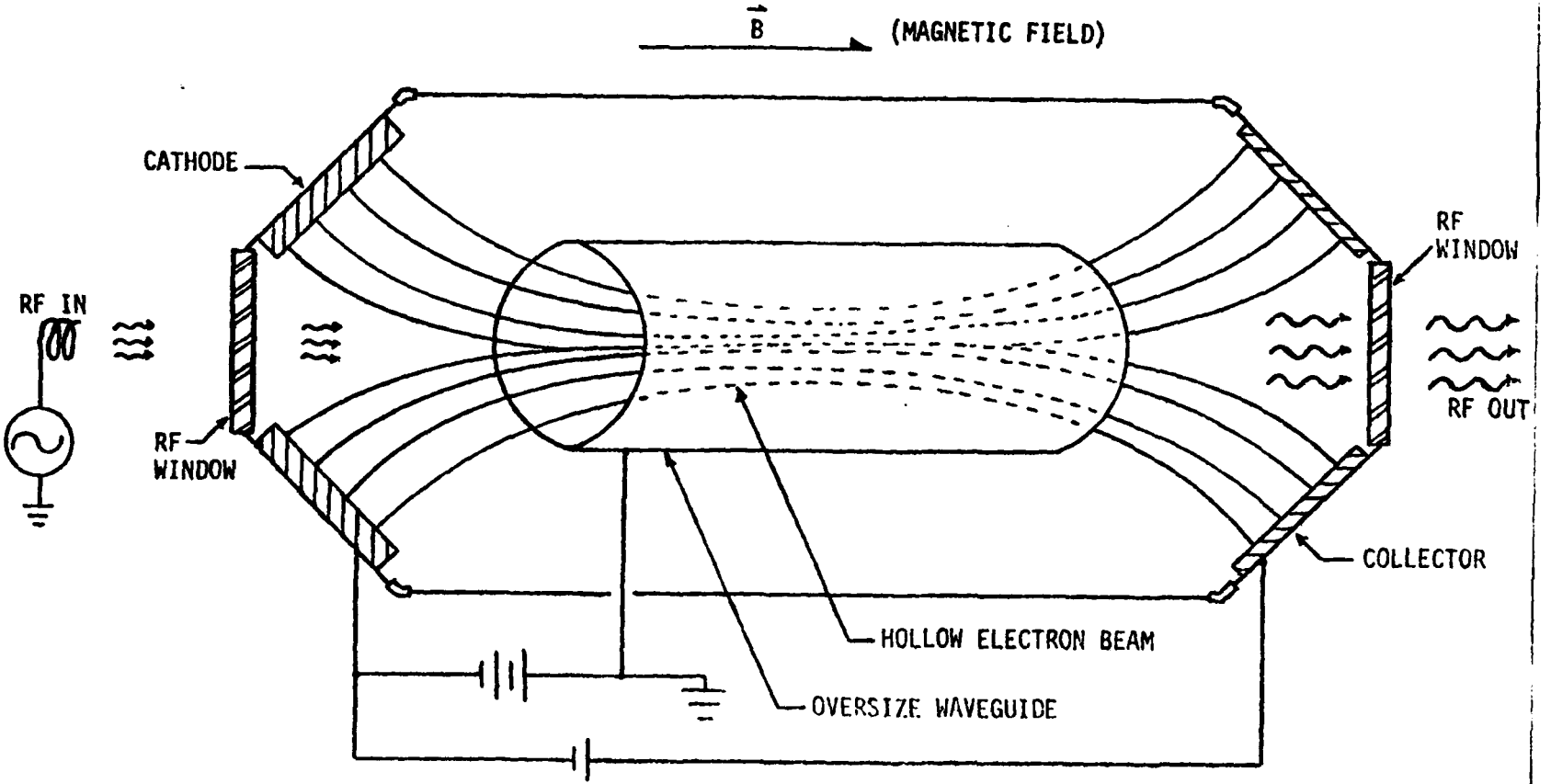

Figure 1. Circuitless Electron Beam Amplifier (CEBA)

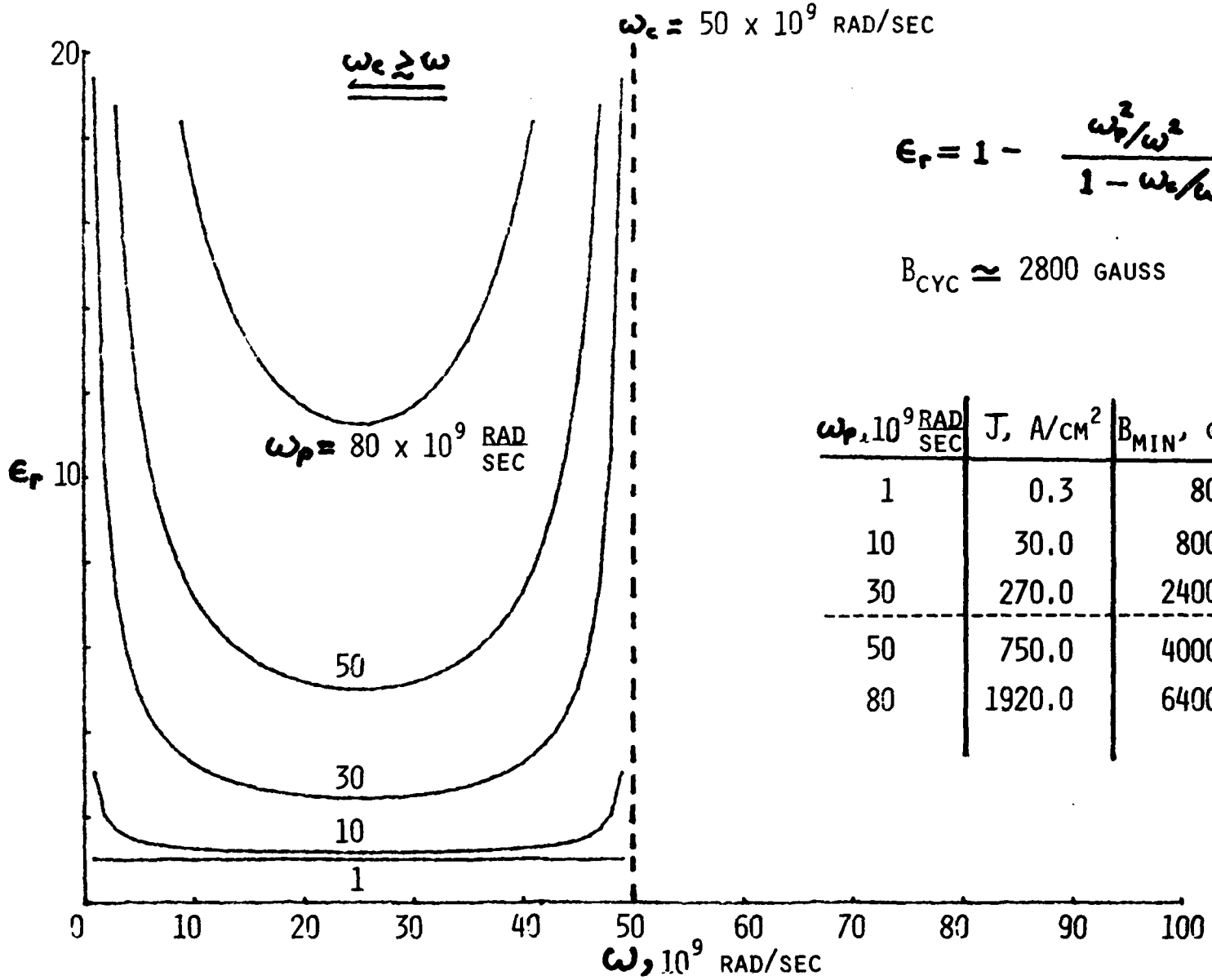

$$\epsilon_r = 1 - \frac{\omega_p^2/\omega^2}{1 - \omega_c/\omega}$$

$B_{CYC} \simeq 2800$ GAUSS

$\omega_p, 10^9 \frac{\text{RAD}}{\text{SEC}}$	J, A/CM^2	B_{MIN}, GAUSS
1	0.3	80
10	30.0	800
30	270.0	2400
50	750.0	4000
80	1920.0	6400

Figure 2. ϵ_r Versus ω For Various Plasma Frequencies and a Given Cyclotron Frequency

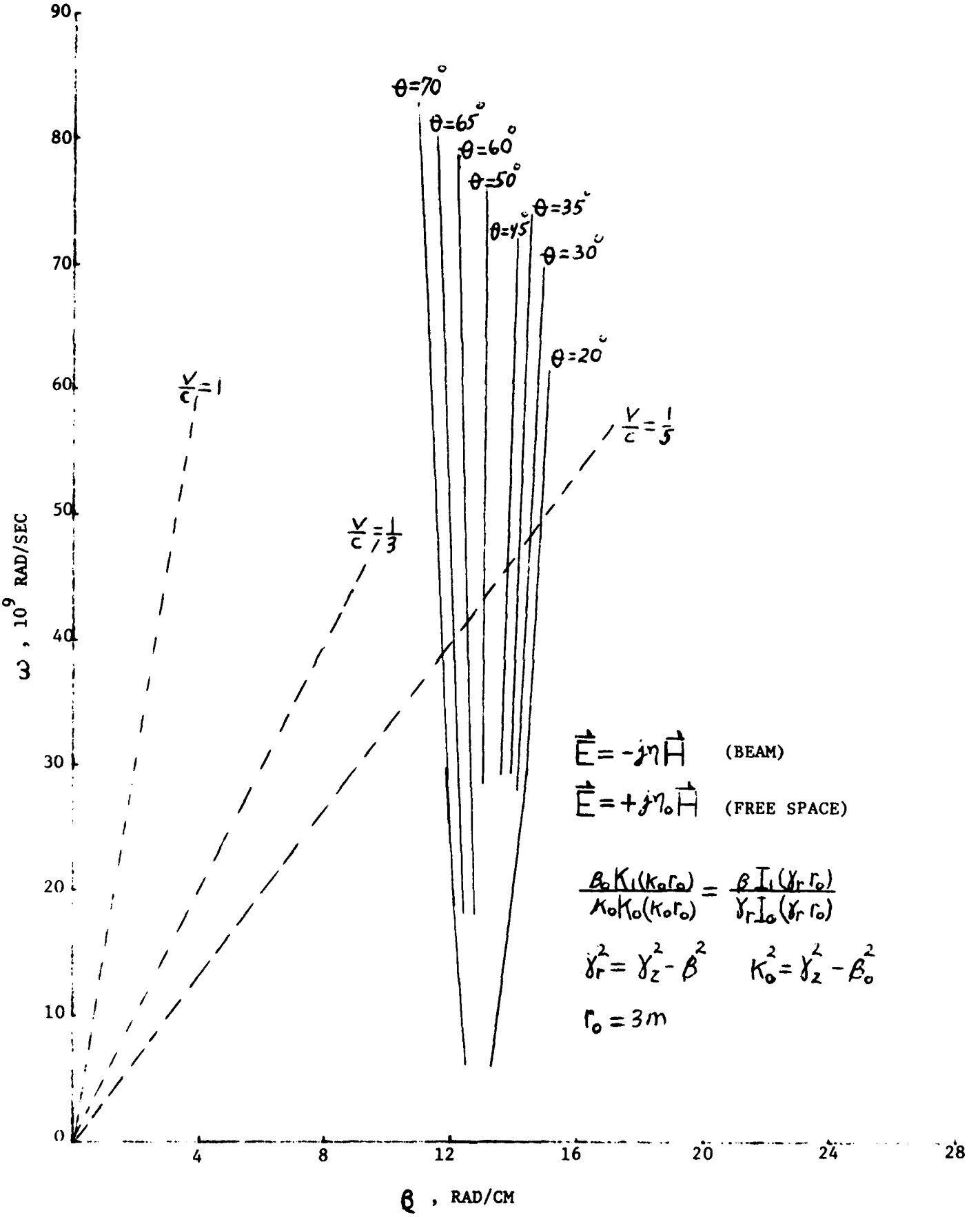

Figure 3. ω Versus β Plot of the Characteristic (Root) Equation

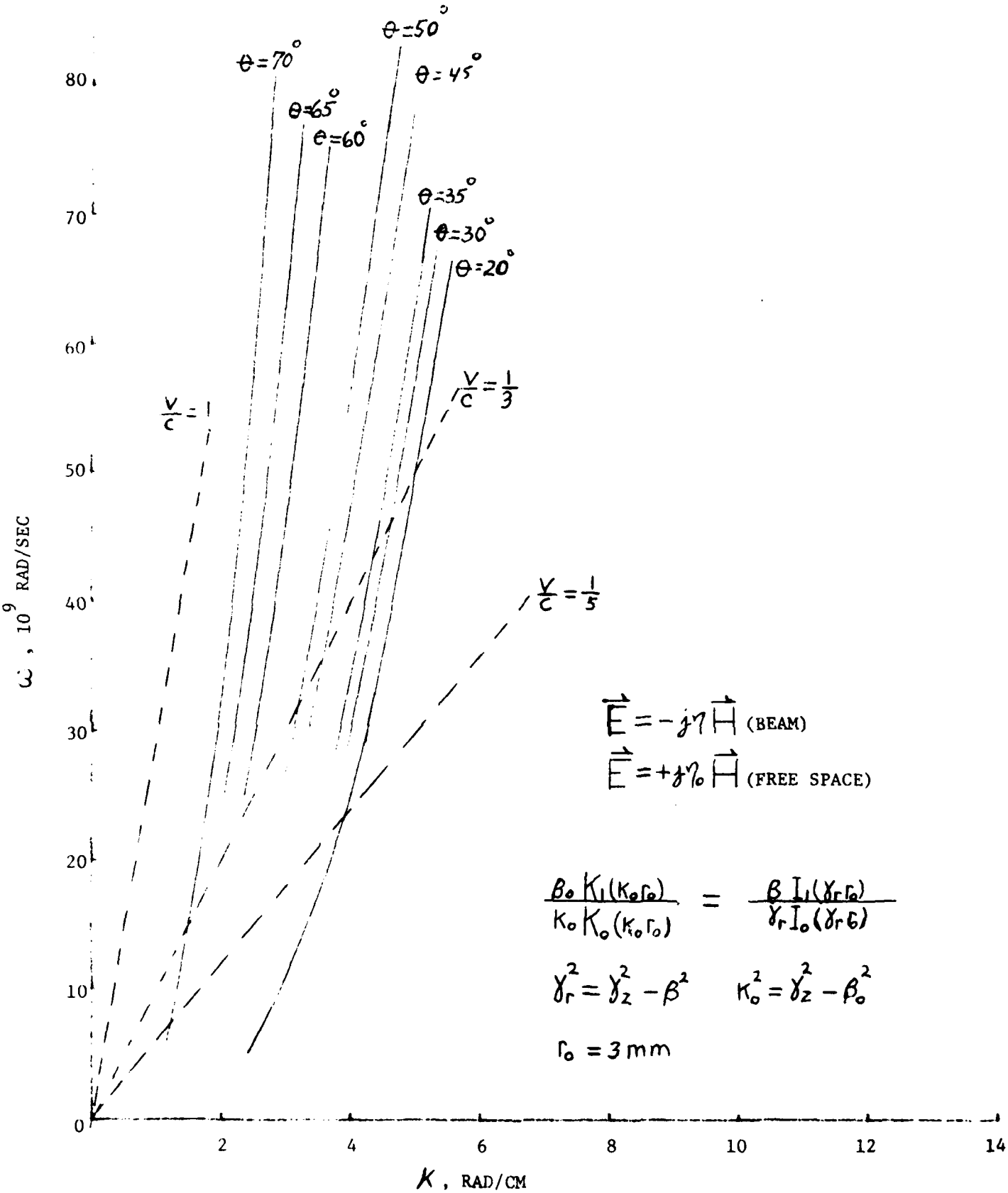

Figure 4. ω Versus K Plot of the Characteristic (Root) Equation

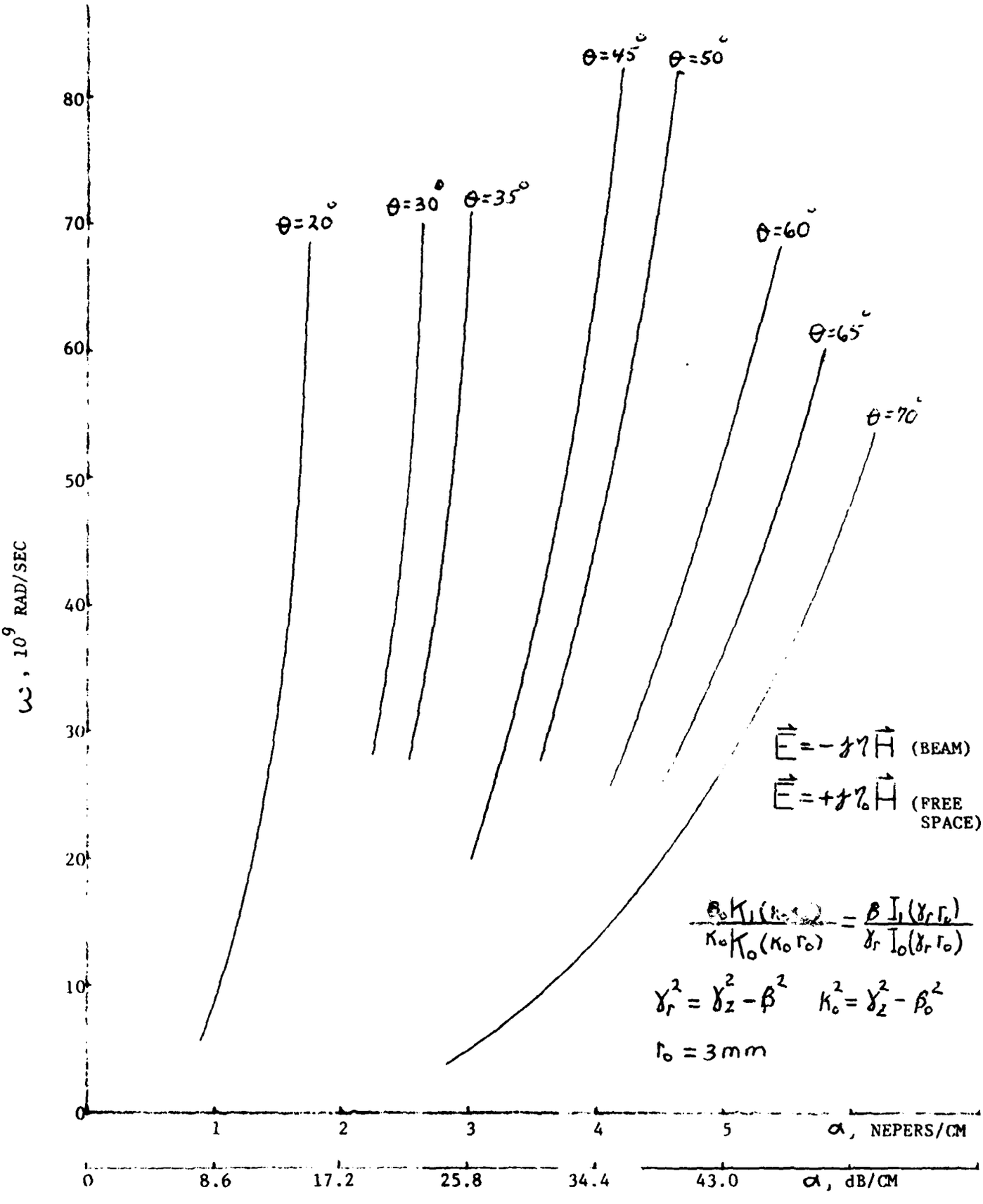

Figure 5. ω Versus α Plot of the Characteristic (Root) Equation

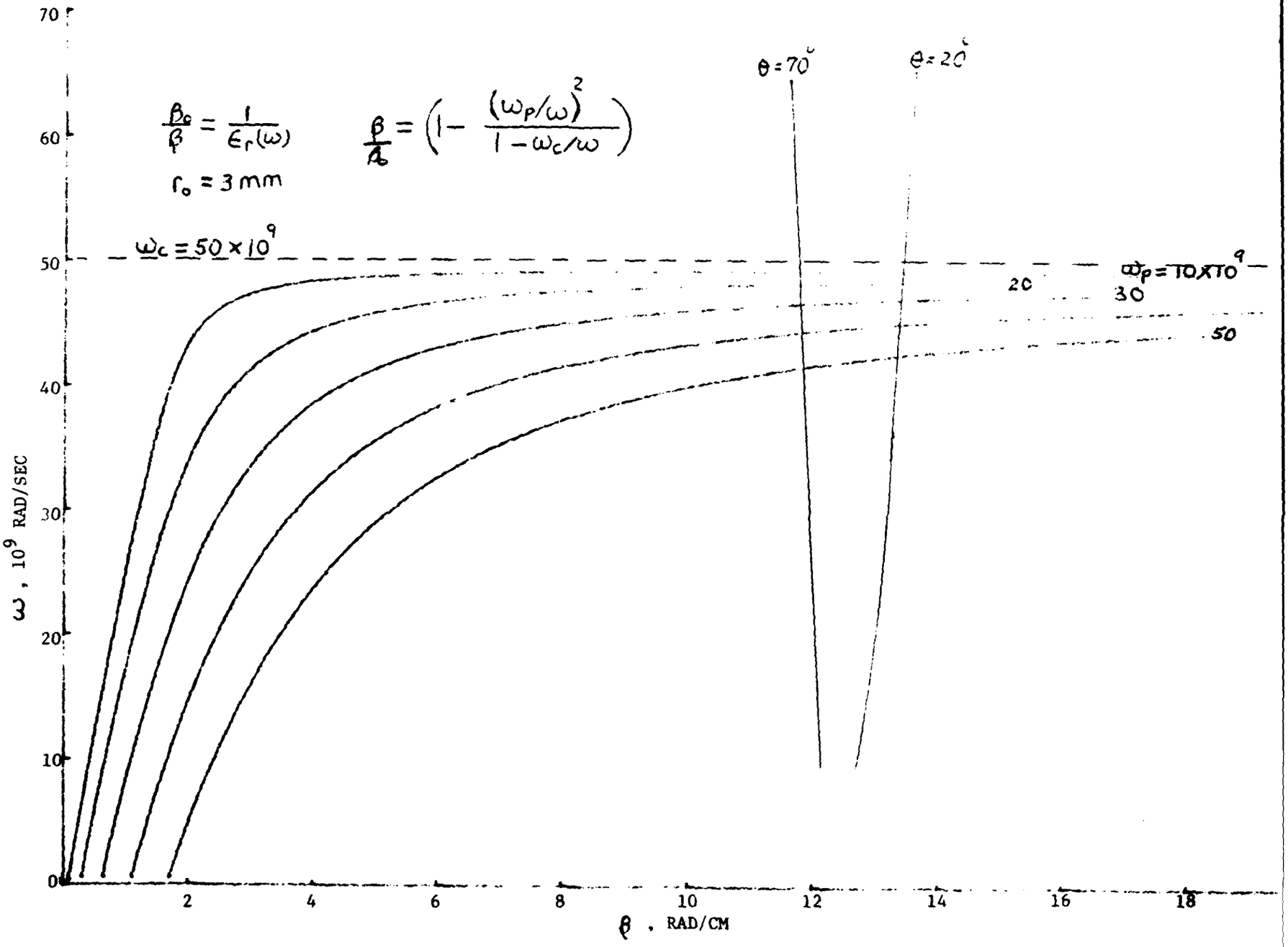

Figure 6. ω Versus β Plot for the Circuitless Electron Beam Amplifier (CEBA)

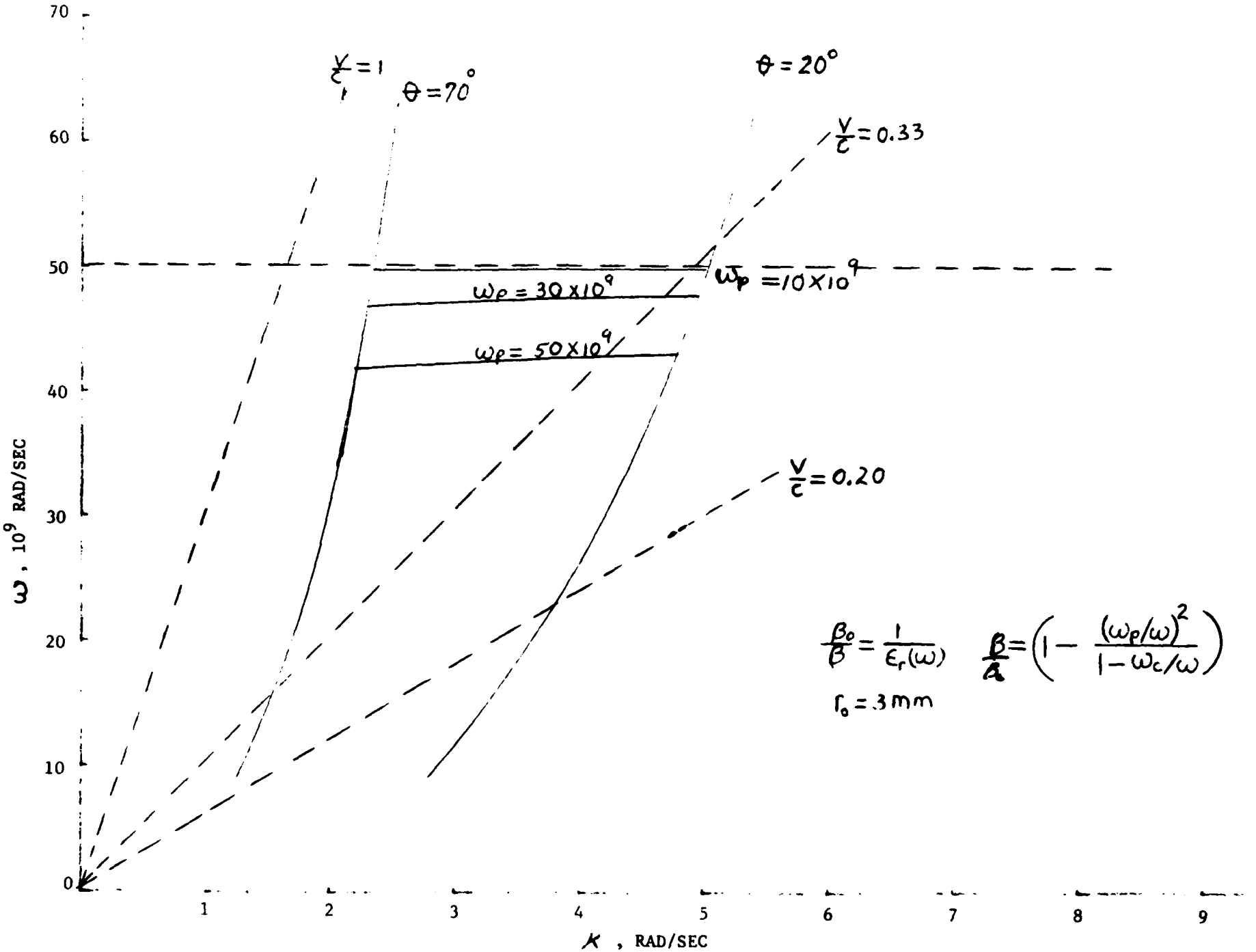

Figure 7. ω Versus K Plot for the Circuitless Electron Beam Amplifier (CEBA)

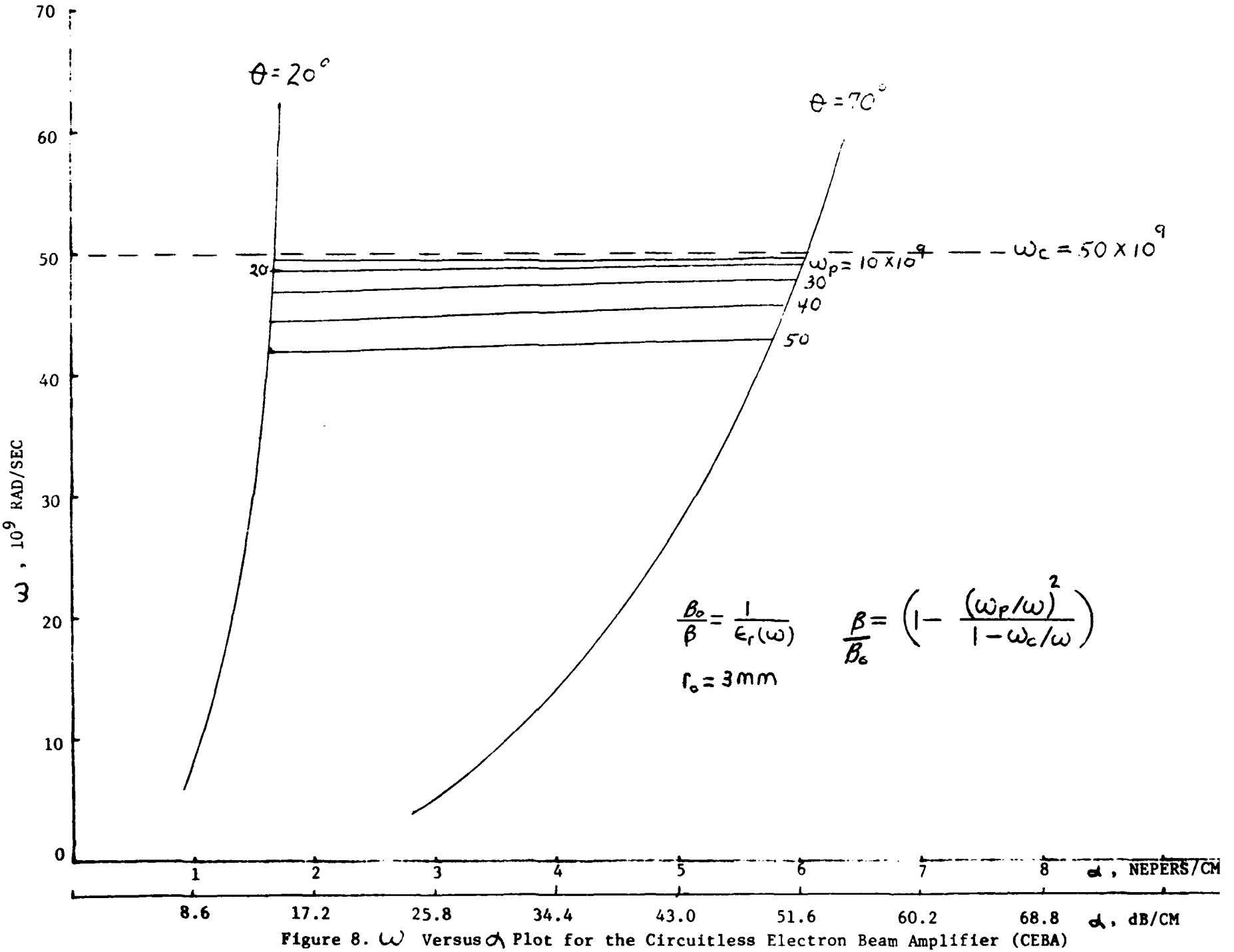

Figure 8. ω Versus α Plot for the Circuitless Electron Beam Amplifier (CEBA)

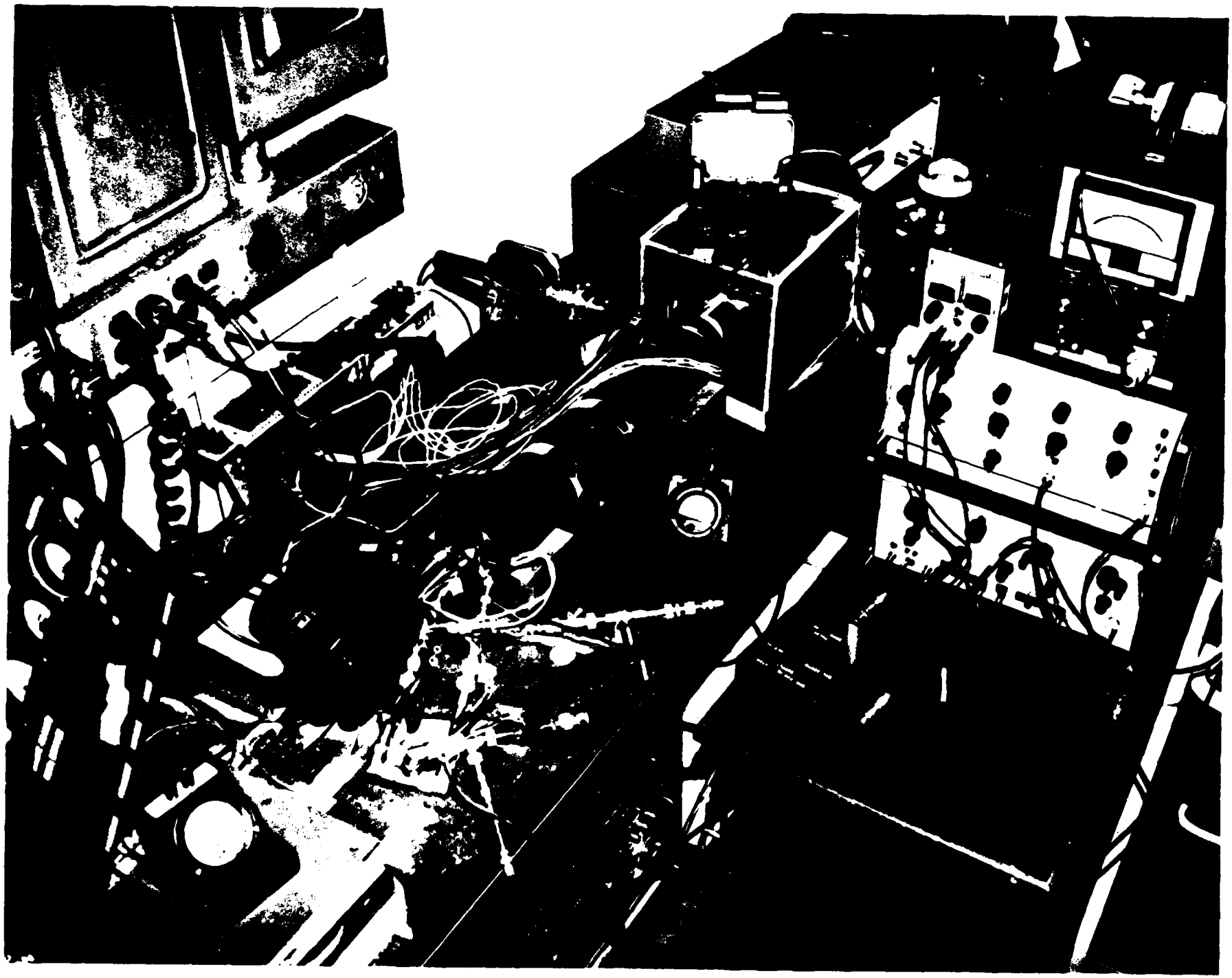

Figure 9. Transverse Wave Traveling-Wave Tube (TWTWT) and Test Equipment

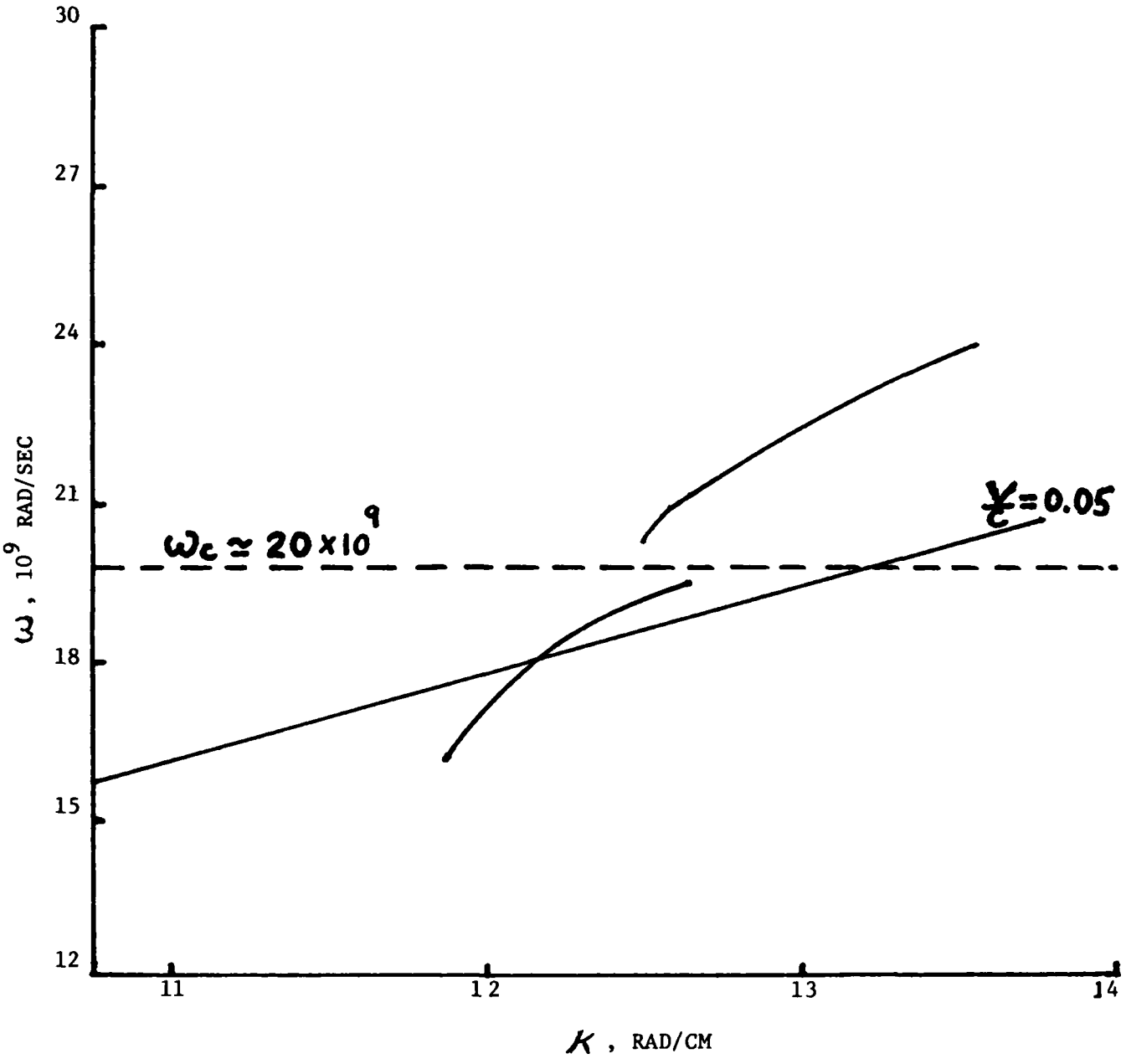

Figure 10. Experimental ω Versus k Plot for the Transverse Traveling-Wave Tube (TWTWT)

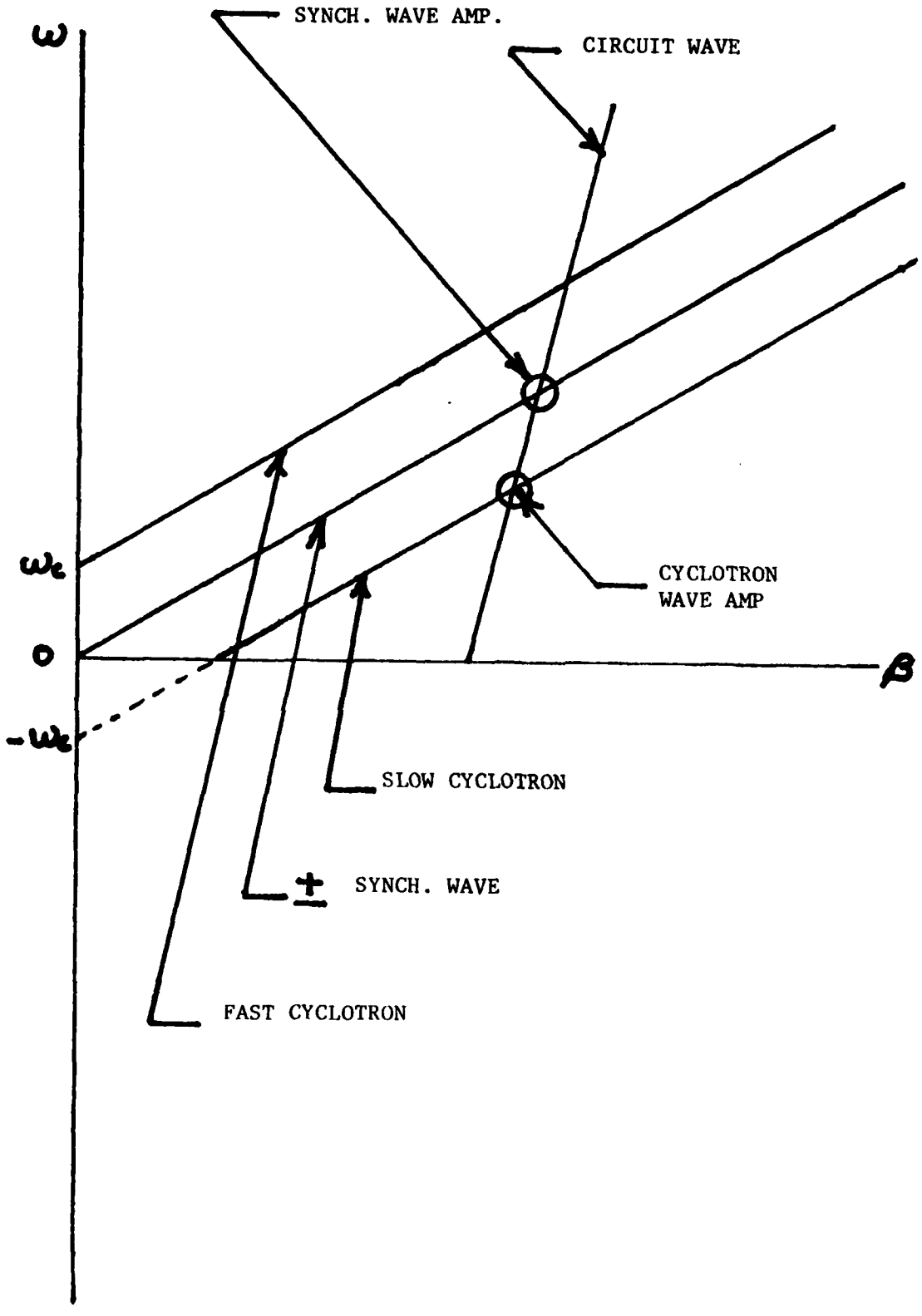

Figure 11. ω Versus β Diagram for the Cyclotron and Synchronous Wave Amplifiers

TABLE 1

Computer Data For The $\theta = 20^\circ$, 45°, and 70° Rays ($r_o = 3\,mm$)

θ°	ξ	ρ	ψ°	$\frac{\beta_o}{\beta}$	N^2	$\epsilon_r(\mu_r)$	$\omega, 10^9 \frac{rad}{sec}$	$\beta, \frac{rad}{cm}$	$K, \frac{rad}{cm}$	α, nepers
20	0.8	3.94	89.24	0.015	15.97	64.94	6.00	13.3	2.44	0.939
20	1.1	4.03	88.63	0.042	17.13	23.81	17.4	13.8	3.46	1.25
20	1.4	4.15	87.90	0.089	18.68	11.24	38.6	14.5	4.55	1.54
20	1.6	4.26	87.40	0.137	20.04	7.30	61.9	15.1	5.38	1.70
20	2.0	4.73	86.71	0.370	25.28	2.70	200	18.0	9.00	1.58
45	1.6	4.05	85.50	0.116	16.16	8.62	46.9	13.5	3.91	3.65
45	2.0	4.15	83.30	0.211	16.79	4.74	88.4	14.0	5.21	4.25
45	2.5	4.45	80.80	0.382	18.79	2.62	179	15.6	7.54	4.60
45	2.7	4.78	80.70	0.508	21.70	1.97	275	18.0	10.0	4.04
70	1.0	3.83	88.75	0.017	13.91	58.14	6.34	12.4	1.15	3.09
70	1.4	3.84	87.55	0.050	13.20	20.00	18.2	12.1	1.61	4.34
70	1.6	3.85	86.81	0.076	12.73	13.16	27.2	11.9	1.84	4.98
70	2.0	3.86	85.02	0.148	11.58	6.76	50.9	11.5	2.35	6.09
70	2.5	3.87	82.20	0.283	9.60	3.53	91.4	10.8	3.05	7.33
70	3.0	3.82	78.35	0.474	6.54	2.11	138	9.68	3.84	8.36

APPENDIX A

Derivation of an Electron Beam with an Isotropic Permittivity ϵ, and/or Permeability μ, in Transverse and Longitudinal dc Magnetic Fields

An electron beam with ϵ and μ identical in all three directions of an orthogonal coordinate system is of importance when solving the wave propagation problem. The authors assume in the solution to Maxwell's equations for RF energy propagating in a dense electron beam that ϵ and μ are scalar quantities. This allows one to readily apply separation of variable techniques and express the field equations as a function of each independent coordinate (r, φ, z). Also Equation (6) $v_p = \frac{c}{\sqrt{\epsilon_r \mu_r}}$ gives the phase velocity of a plane wave in terms of the scalar quantities ϵ_r and μ_r.

The derivation for the isotropic dielectric constant or an electron beam in a magnetic field is presented below. The analysis for the permeability μ is identical and, therefore, will not be given here.

Let

$$\vec{V} = V_1 \hat{e}_1 \pm j V_2 \hat{e}_2 + V_3 \hat{e}_3$$

$$\vec{B} = B_0 (B_1 \hat{e}_1 + B_2 \hat{e}_2 + B_3 \hat{e}_3) \qquad \text{(A-1)}$$

$$\vec{E} = E_0 (A_4 \hat{e}_1 \pm j A_5 \hat{e}_2 + A_6 \hat{e}_3)$$

where $\hat{e}_1$, $\hat{e}_2$ and $\hat{e}_3$ are unit vectors and $\vec{V}$ and $\vec{E}$ describe alternating current (ac) velocity components of the electron beam and RF field components respectively. The vectors $\vec{V}$ and $\vec{E}$ are expressed with vector components of different amplitudes and phases to give transverse elliptical polarization. The magnetic field $\vec{B}$ consists only of dc components. The The ac components of the magnetic field are neglected since for non-relativistic velocities, the self generated magnetic fields of the electrons are negligible compared to the applied fields. When the amplitude of the electronic motion of the electrons is small and collisions are neglected, the equation of motion is approximately:[12]

$$m \frac{d\vec{V}}{dt} \simeq -e\vec{E} e^{j\omega t} - e(\vec{V} \times \vec{B}) \qquad \text{(A-2)}$$

The Lorentz equation (equation of motion) expressed in component vector form gives:

$$j\omega m \begin{vmatrix} V_1 \hat{e}_1 \\ \pm j V_2 \hat{e}_2 \\ V_3 \hat{e}_3 \end{vmatrix} = -eE_0 \begin{vmatrix} A_4 \hat{e}_1 \\ \pm j A_5 \hat{e}_2 \\ A_6 \hat{e}_3 \end{vmatrix} \mp j e B_0 \begin{vmatrix} (V_2 B_3 \pm j V_3 B_2) \hat{e}_1 \\ \pm j (V_1 B_3 - V_3 B_1) \hat{e}_2 \\ (\mp j V_1 B_2 - V_2 B_1) \hat{e}_3 \end{vmatrix} \qquad \text{(A-3)}$$

12 J. Jackson, "Classical Electrodynamics," John Wiley & Sons, p 228,1962.

where differentiation with respect to time of a sinusoidal disturbance yields $j\omega$. From Equation (A-3), the three velocity components are:

$$\hat{e}_1: \quad V_1 = \frac{j\eta_e E_o A_4}{\omega(1 \pm \omega_c/\omega)} \quad \text{for} \quad V_1 \triangleq V_2 B_3 \pm j B_2 V_3 \tag{A-4}$$

$$\hat{e}_2: \quad V_2 = \frac{j\eta_e E_o A_5}{\omega(1 \pm \omega_c/\omega)} \quad \text{for} \quad V_2 \triangleq V_1 B_3 - V_3 B_1 \tag{A-5}$$

$$\hat{e}_3: \quad V_3 = \frac{j\eta_e E_o A_6}{\omega(1 \pm \omega_c/\omega)} \quad \text{for} \quad V_3 \triangleq \mp j V_1 B_2 - V_2 B_1 \tag{A-6}$$

The curl $\vec{H}$ expressed in vector form is:

$$\nabla \times \vec{H} = j\omega\epsilon_o \vec{E} + \vec{J} = j\omega\epsilon_o \vec{E} - \rho_o \vec{V}$$

or

$$\nabla \times \vec{H} = j\omega\epsilon_o E_o \begin{vmatrix} A_4\hat{e}_1 \\ \pm jA_5\hat{e}_2 \\ A_6\hat{e}_3 \end{vmatrix} - \rho_o \begin{vmatrix} V_1\hat{e}_1 \\ \pm jV_2\hat{e}_2 \\ V_3\hat{e}_3 \end{vmatrix} \tag{A-7}$$

where ρ_o is the charge density.

From Equations (A-4) through (A-7), the curl $\vec{H}$ vector components are:

$$(\nabla \times \vec{H})\hat{e}_1 = j\omega\epsilon_o \left[1 - \frac{(\omega_p/\omega)^2}{1 \pm \omega_c/\omega}\right] E_o A_4 = j\omega\epsilon_o\epsilon_r E_o A_4 \tag{A-8}$$

$$(\nabla \times \vec{H})\hat{e}_2 = \mp j\omega\epsilon_o \left[1 - \frac{(\omega_p/\omega)^2}{1 \pm \omega_c/\omega}\right] E_o A_5 = \mp j\omega\epsilon_o\epsilon_r E_o A_5 \tag{A-9}$$

$$(\nabla \times \vec{H})\hat{e}_3 = j\omega\epsilon_o \left[1 - \frac{(\omega_p/\omega)^2}{1 \pm \omega_c/\omega}\right] E_o A_6 = j\omega\epsilon_o\epsilon_r E_o A_6 \tag{A-10}$$

where $\omega_p^2 = \frac{\rho_0 \eta_e}{\epsilon_0}$.

As can be seen, Equations (A-8) through (A-10) yield an isotropic permittivity ϵ, ($\epsilon_0 \epsilon_r = \epsilon$).

Examining the conditions required for an isotropic dielectric beam as given by the velocity-magnetic field relationships of Equations (A-4) through (A-6), one can form ratios of the velocity components

$$\frac{V_2}{V_1} = \left[\frac{B_3 \pm j B_1 B_2}{1 - B_1^2}\right] \quad \text{and} \quad \frac{V_3}{V_1} = \left[\frac{\mp j B_2 - B_1 B_3}{1 - B_1^2}\right] \qquad \text{(A-11)}$$

where

$$B_1^2 + B_2^2 + B_3^2 = 1$$

The above equation indicates that in order to have a velocity component V_3, at least one transverse dc magnetic field component (B_1 or B_2) must exist.

If $B_3 = 1$, $B_1 << 1$, and $B_2 << 1$ then $V_2/V_1 \simeq 1$ and $V_3/V_1 \simeq -B_1$.

Under these approximate conditions, the transverse velocity components are circularly polarized.

When one uses an axial current carrying wire in the CEBA to generate a small magnetic field B_φ, then one can apply the conditions $B_1 = 0$,

$B_2 \triangleq B_\varphi << 1$, and $B_3 = 1$. Thus $\frac{V_2}{V_1} = 1$ and $\frac{V_3}{V_1} = \mp j B_\varphi$.

Under these approximate conditions, the transverse velocity components are also circularly polarized. It is shown in Appendix C, that the field equations, in the electron beam region, can be expressed as modified Bessel functions of the first kind with complex arguments where:

$$E_r \triangleq E_1 \propto A_4 \propto + j \frac{\gamma_z}{\gamma_r} I_1(\gamma_r r)$$

$$E_\varphi \triangleq E_2 \propto \pm j A_5 \propto + \frac{\beta}{\gamma_r} I_1(\gamma_r r) \quad \text{or} \quad A_5 \propto \mp j \frac{\beta}{\gamma_r} I_1(\gamma_r r) \qquad \text{(A-12)}$$

$$E_z \triangleq E_3 \propto A_6 \propto I_0(\gamma_r r)$$

where $\beta = \omega\sqrt{\epsilon\mu}$, $\gamma_r^2 = \gamma_z^2 - \beta^2$, and γ_r and γ_z are the complex

radial and longitudinal propagation constants respectively. Using Equations (A-4) through (A-6) and applying Equations (A-12) give

$$\frac{V_2}{V_1} = \frac{A_5}{A_4} = \mp \frac{\beta}{\gamma_z} \quad \text{and} \quad \frac{V_3}{V_1} = \frac{A_6}{A_4} = -j \frac{\gamma_r}{\gamma_z} \frac{I_0(\gamma_r r)}{I_1(\gamma_r r)} \tag{A-13}$$

Using Equations (A-11) and (A-13) for $B_1 = 0$ gives

$$B_3 = \mp \frac{\beta}{\gamma_z} \quad \text{and} \quad B_2 = \pm \frac{\gamma_r}{\gamma_z} \frac{I_0(\gamma_r r)}{I_1(\gamma_r r)} \tag{A-14}$$

Note, that in Equation (A-14), $I_1(\gamma_r r) \to 0$ as $r \to 0$ (gives a pole).

For small r, the ratio $I_0(\gamma_r r) / I_1(\gamma_r r) \propto 1/\gamma_r r$.

Similarily, the magnetic field around a current carrying axial wire is proportional to $1/r$. Thus, the axial current carrying wire is a reasonable approximation to the required magnetic field in the φ direction for small r. Considering Equations (A-14)

for: $\gamma_z = \kappa + j\alpha$, κ and $\beta >> \alpha$ and $I_0(\gamma_r r)/I_1(\gamma_r r) \simeq \frac{2}{\gamma_r r}$

then $B_3 \simeq \mp \frac{\beta}{\kappa}$ and $B_2 \simeq \pm \frac{2}{\kappa r}$. (A-15)

APPENDIX B

Derivation of an Electron Beam with an Isotropic Permittivity ϵ, and/or Permeability μ, in a Longitudinal dc Magnetic Field

This method of deriving an isotropic permittivity ϵ, is similar to the derivation of the isotropic ϵ given in Appendix A. However, for this method, only a dc magnetic field in the z direction is required. Also, the derivative of the ac component of the velocity is given as:

$$\frac{dv}{dt} = \frac{\partial v}{\partial t} + \frac{\partial v}{\partial z}\frac{dz}{dt} \tag{B-1}$$

where $\frac{dz}{dt} = u_0$ and u_0 is the average electron velocity in the z direction. Note that $\frac{\partial v_1}{\partial z}$ and $\frac{\partial v_2}{\partial z}$ are neglected in this approximation.

Applying the Lorentz equation and expressing partial derivatives with respect to time and distance as $\frac{\partial v_N}{\partial t} = j\omega v_N$ for $N = 1, 2, 3$ and $\frac{\partial v_3}{\partial z}\frac{dz}{dt} = -j\gamma_z u_0 v_3$, then the three velocity components are:

$$v_1 = \frac{j\eta_e E_0 A_4}{\omega(1 \pm \omega_c/\omega)} \quad \text{for} \quad v_1 \simeq v_2 \tag{B-2}$$

$$v_2 = \frac{j\eta_e E_0 A_5}{\omega(1 \pm \omega_c/\omega)} \quad \text{for} \quad v_1 \simeq v_2 \tag{B-3}$$

$$v_3 = \frac{j\eta_e E_0 A_6}{\omega(1 \pm \omega_c/\omega)} \quad \text{for} \quad \gamma_z u_0 = \pm\omega_c \tag{B-4}$$

The three curl $\vec{H}$ components listed below give the isotropic ϵ for the conditions that $v_1 \simeq v_2$, $\gamma_z = \kappa + j\alpha \simeq \kappa$ (for $\kappa >> \alpha$), and $\kappa u_0 \simeq \omega_c$

$$(\nabla \times \vec{H})_{\hat{e}_1} = j\omega\epsilon_0\left[1 - \frac{(\omega_p/\omega)^2}{1 \pm \omega_c/\omega}\right]E_0 A_4 = j\omega\epsilon_0\epsilon_r E_0 A_4 \tag{B-5}$$

$$(\nabla \times \vec{H})\hat{e}_2 = \mp \omega \epsilon_0 \left[1 - \frac{(\omega_p/\omega)^2}{1 \pm \omega_c/\omega}\right] E_0 A_5 = \mp \omega \epsilon_0 \epsilon_r E_0 A_5 \quad \text{(B-6)}$$

$$(\nabla \times \vec{H})\hat{e}_3 = j\omega \epsilon_0 \left[1 - \frac{(\omega_p/\omega)^2}{1 \pm \omega_c/\omega}\right] E_0 A_6 = j\omega \epsilon_0 \epsilon_r E_0 A_6 \quad \text{(B-7)}$$

Therefore, relative permittivity, $\epsilon_r \triangleq \left[1 - \frac{(\omega_p/\omega)^2}{1 \pm \omega_c/\omega}\right]$

In a like manner it can be shown that the relative permeability

$\mu_r \triangleq \left[1 - \frac{(\omega_p/\omega)^2}{1 \pm \omega_c/\omega}\right]$, under the condition that both the electric and magnetic current densities exist and are related by Equation (7).

APPENDIX C

Derivation of the Electromagnetic (EM) Field Expressions and Transcendental Root Equation for Propagation Through an Active Dielectric Medium (Solid Cylindrical Electron Beam)

The system considered is a solid electron beam traveling inside an oversized waveguide with RF energy propagating through the electron beam. The solid electron beam is an approximation to the converging electron beam as depicted in Figure 1 (CEBA). This being the case, consider the system as shown:

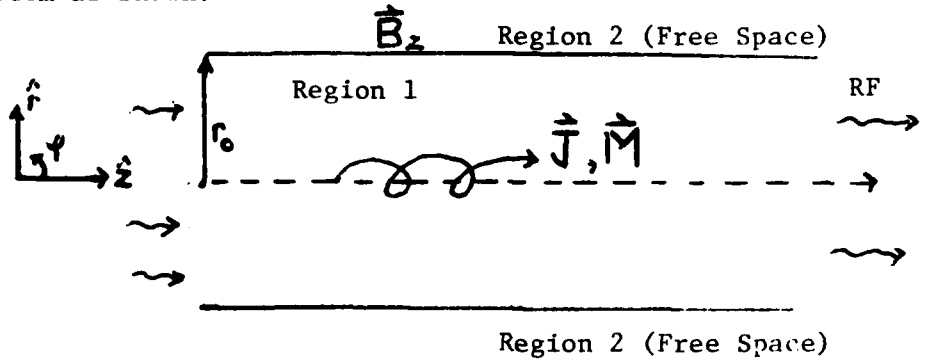

The cylindrical coordinate system is used.

The EM fields have the form:

$$E, H \propto A(r,\varphi)\, e^{j(\omega t - \gamma_z z + N\varphi)}$$

where

$$A(r,\varphi) = \begin{cases} J_N(\gamma_r r) \text{ or } I_N(\gamma_r r) & r \le r_0 \\ K_N(\kappa_0 r) & r \ge r_0 \end{cases} \qquad \text{(C-1)}$$

$J_N(\gamma_r r)$, $I_N(\gamma_r r)$, and $K_N(\kappa_0 r)$ are Bessel functions;

γ_r and κ_0 are complex radial propagation constants;

γ_z is the complex longitudinal propagation constant ($\gamma_z = \kappa + j\alpha$);

and $N = 0, \pm 1, \pm 2, \pm 3 \text{ ----}$.

The problem was solved for $A(r,\varphi) = J_N(\gamma_r r)$ and $A(r,\varphi) = I_N(\gamma_r r)$.

Roots of the boundary value problem exist for both cases. However, in order to have an isotropic ϵ_r, $\beta \simeq \kappa >> \alpha$. This condition was better satisfied for $A(r,\varphi) = I_N(\gamma_r r)$ then for $A(r,\varphi) = J_N(\gamma_r r)$. The derivation of

the field expressions will be for $A(r,\varphi) = I_N(\gamma_r r)$ and $K_N = (\kappa_0 r)$ where $\gamma_r^2 = \gamma_z^2 - \beta^2$ and $\kappa_0^2 = \gamma_z^2 - \beta_0^2$.

Maxwell's equations for the present problem are:

$$\nabla \times \vec{E} = -\frac{\partial \vec{B}}{\partial t} \; ; \quad \nabla \times \vec{H} = \frac{\partial \vec{D}}{\partial t} \; ; \quad \nabla \cdot \vec{D} = 0 ; \quad \nabla \cdot \vec{B} = 0 ; \qquad \text{(C-2)}$$

and $\nabla \cdot \vec{J} = -\frac{\partial \rho}{\partial t}$.

The electric and magnetic sources are included in $\vec{B}$ and $\vec{D}$ as

$$\vec{D} = \epsilon_0(1 + \chi_E)\vec{E} = \epsilon \vec{E} \quad \text{and} \quad \vec{B} = \mu_0(1 + \chi_M)\vec{H} = \mu \vec{H} \quad \text{where}$$
$$\vec{J} = j\omega \epsilon_0 \chi_E \vec{E} \quad \text{and} \quad \vec{M} = -j\omega \mu_0 \chi_M \vec{H} \qquad \text{(C-3)}$$

The relationships between the $\vec{E}$ and $\vec{H}$ fields and $\vec{J}$ and $\vec{M}$ sources are:

$\vec{E} = -j\eta \vec{H}$ (beam), $\vec{E} = j\eta_0 \vec{H}$ (free space), and

$\vec{M} = -j\eta \vec{J}$ where $\eta = \sqrt{\mu/\epsilon}$ and $\eta_0 = \sqrt{\mu_0/\epsilon_0}$

The EM field expressions (in region 1) are derived from the r, φ, z components of the curl $\vec{E}$ and curl $\vec{H}$ equations. Six differential equations are obtained and these are listed below:

$$E_z'' + \frac{1}{r} E_z' + \left(-\gamma_r^2 - \frac{N^2}{r^2}\right) E_z = 0$$
$$H_z'' + \frac{1}{r} H_z' + \left(-\gamma_r^2 - \frac{N^2}{r^2}\right) H_z = 0$$

Wave equations satisfied by modified Bessel functions

(C-4)

$$H_\varphi = -\frac{jN\gamma_z}{\eta \gamma_r^2 r} E_z + \frac{j\omega\epsilon}{\gamma_r^2} E_z'$$

$$E_r = -\frac{jN\omega\mu}{\eta \gamma_r^2 r} E_z + \frac{j\gamma_z}{\gamma_r^2} E_z'$$

$$H_r = \frac{N\omega\epsilon}{\gamma_r^2 r} E_z - \frac{\gamma_z}{\eta \gamma_r^2} E_z'$$

$$E_\varphi = -\frac{N\gamma_z}{\gamma_r^2 r} E_z + \frac{\omega\mu}{\eta \gamma_r^2} E_z'$$

E'' and H'' implies $\frac{\partial^2}{\partial r^2}E$ and $\frac{\partial^2}{\partial r^2}H$. Likewise E' and H' implies $\frac{\partial}{\partial r}E$ and $\frac{\partial}{\partial r}H$.

The authors, presently, have limited the investigation to the $N=0$ order modes. For $N=0$, the E_r, E_φ and H_r, H_φ are nearly circular polarized since

$$\frac{E_r}{E_\varphi}=j\frac{\gamma_z}{\beta} \quad \text{and} \quad \frac{H_r}{H_\varphi}=j\frac{\gamma_z}{\beta}$$. When $\kappa >> \alpha$ then

$$\frac{E_r}{E_\varphi}=j\frac{\kappa}{\beta} \quad \text{and} \quad \frac{H_r}{H_\varphi}=j\frac{\kappa}{\beta}.$$

The EM field expressions for region 1 and 2 are given below where the term $\exp[j(\omega t-\gamma_z z)]$ is understood to be present for each field. Note, that the EM field expressions for region 2 are derived in like manner to the derivation of the fields in region 1.

Region 1 (Electron Beam)

$$E_{1z}=C_1 I_0(\gamma_r r)\ ; \quad E_{1r}=\frac{j\gamma_z}{\gamma_r}C_1 I_1(\gamma_r r)\ ; \quad E_{1\varphi}=\frac{\omega\mu}{\eta\gamma_r}C_1 I_1(\gamma_r r)\ ; \quad \text{(C-5)}$$

$$H_{1z}=\frac{j}{\eta}C_1 I_0(\gamma_r r)\ ; \quad H_{1r}=-\frac{\gamma_z}{\eta\gamma_r}C_1 I_1(\gamma_r r)\ ; \quad H_{1\varphi}=\frac{j\omega\epsilon}{\gamma_r}C_1 I_1(\gamma_r r);$$

where $\vec{E}=-j\eta\vec{H}$, $\gamma_r^2=\gamma_z^2-\beta^2$, $\eta=\sqrt{\mu/\epsilon}$,

$\beta=\omega\sqrt{\epsilon\mu}$, and $\gamma_z=\kappa+j\alpha$.

Region 2 (Free Space)

$$E_{2z}=C_2K_0(\kappa_0 r);\quad E_{2r}=\frac{-j\gamma_z}{\kappa_0}C_2K_1(\kappa_0 r);\quad E_{2\varphi}=\frac{\omega\mu_0}{\gamma_0\kappa_0}C_2K_1(\kappa_0 r);$$

$$H_{2z}=\frac{-j}{\gamma_0}C_1K_0(\kappa_0 r);\quad H_{2r}=\frac{-\gamma_z}{\gamma_0\kappa_0}C_2K_1(\kappa_0 r);\quad H_{2\varphi}=\frac{-j\omega\epsilon_0}{\kappa_0}C_2K_1(\kappa_0 r); \tag{C-6}$$

where $\vec{E}=j\eta\vec{H}$, $\kappa_0^2=\gamma_z^2-\beta_0^2$, $\eta_0=\sqrt{\mu_0/\epsilon_0}$, $\beta_0=\omega\sqrt{\epsilon_0\mu_0}$,

and $\gamma_z=\kappa+j\alpha$

The characteristic (root) equation is obtained by specifying that at the beam radius r_0, the tangential fields must be continuous. The boundary conditions are:

$$H_{TAN_1}=H_{TAN_2}\quad\text{and}\quad E_{TAN_1}=E_{TAN_2}$$

or

$$E_{1z}=E_{2z},\quad E_{1\varphi}=E_{2\varphi}\ \text{and}\ H_{1\varphi}=H_{2\varphi} \tag{C-7}$$

However, the E_φ and H_φ equations are equivalent so that two equations exist with two unknown arbitrary coefficients C_1 and C_2. Equating the determinant to zero gives:

$$\frac{\beta I_1(\gamma_r r_0)}{\gamma_r I_0(\gamma_r r_0)}=\frac{\beta_0 K_1(\kappa_0 r_0)}{\kappa_0 K_0(\kappa_0 r_0)} \tag{C-8}$$

Equation (C-8) is separated into real and imaginary parts. First, consider the left-hand side of Equation (C-8)

$$\frac{\beta I_1(\gamma_r r_0)}{\gamma_r I_0(\gamma_r r_0)}$$

where the $I_N(\gamma_r r_0)$ are transformed into $J_N(\gamma_r r_0)$ functions.[13] The transformation from modified Bessel functions I_N and K_N into J_N and Y_N were made because the series expansions for the J_N functions

13 Handbook of Mathematical Functions with Formulas, Graphs, and Mathematical Tables," US Department of Commerce, NBS, pp. 355-436, June 1964.

are much simpler to program into the computer and tables of tabulated values are available in literature.[14,15]

Let $\gamma_r r_o = \rho e^{j\Psi}$, $I_o(\gamma_r r_o) = J_o(\rho, e^{j(\varphi + \pi/2)})$

and $I_1(\gamma_r r_o) = -jJ_1(\rho, e^{j(\varphi + \pi/2)})$ for $(-\pi < \arg(\gamma_r r_o) \leq \frac{\pi}{2})$

The ratio $$\frac{I_1(\gamma_r r_o)}{I_o(\gamma_r r_o)} = -j \frac{[\mathrm{Re}\, J_1(\rho,\tau) + j[\mathrm{Im}\, J_1(\rho,\tau)]}{[\mathrm{Re}\, J_o(\rho,\tau) + j\mathrm{Im}\, J_o(\rho,\tau)]} \qquad \text{(C-9)}$$

where $\tau = \varphi + \frac{\pi}{2}$. Using the notation given in Reference 14.

$$J_o(\rho,\tau) = U_o(\rho,\tau) + jV_o(\rho,\tau) \qquad \text{and}$$

$$J_1(\rho,\tau) = U_1(\rho,\tau) + jV_1(\rho,\tau)$$

Equation (C-9) becomes:

$$\frac{I_1(\gamma_r r_o)}{I_o(\gamma_r r_o)} = -j \frac{[(U_1U_o + V_1V_o) - (U_1V_o - U_oV_1)]}{U_o^2 + V_o^2} \qquad \text{(C-10)}$$

Let $A = U_o(\rho,\tau)U_1(\rho,\tau) + V_o(\rho,\tau)V_1(\rho,\tau)$

$B = U_1(\rho,\tau)V_o(\rho,\tau) - U_o(\rho,\tau)V_1(\rho,\tau)$ and

The left-hand side of Equation (C-8) becomes:

$$\frac{\beta I_1(\gamma_r r_o)}{\gamma_r I_o(\gamma_r r_o)} = \frac{-\beta r_o}{\rho}\left[\frac{(A\,\mathrm{SIN}(\varphi) + B\,\mathrm{COS}(\varphi)) + j(A\,\mathrm{COS}(\varphi) - B\,\mathrm{SIN}(\varphi))}{U_o^2(\rho,\tau) + V_o^2(\rho,\tau)}\right] \qquad \text{(C-11)}$$

The right-hand side of Equation (C-8) is represented in a similar manner.[16,17]

Let $\kappa_o r_o = \xi e^{j\theta}$, $K_o(\kappa_o r_o) = -\frac{\pi}{2}[Y_o(\xi, e^{j(\pi/2+\theta)}) - jJ_o(\xi, e^{j(\pi/2+\theta)})]$

---

14 Table of Bessel Functions - Op. Cit #8
15 Table of Bessel Functions - Op. Cit #9
16 Handbook of Mathematical Functions - Op. Cit #13
17 Table of Bessel Functions - Op. Cit #9

and $K_1(\kappa_0 r_0) = -\frac{\pi}{2}\left[j Y_1(\xi, e^{j(\pi/2+\theta)}) + J_1(\xi, e^{j(\pi/2+\theta)})\right]$

for $(-\pi < \arg(\kappa_0 r_0) \leq \pi/2)$

Using the following notation gives:

$(\theta + \pi/2) = \phi$, $U_0 = Re(J_0)$, $U_1 = Re(J_1)$, $V_0 = Imq(J_0)$, $V_1 = Imq(J_1)$,

$W_0 = Re(Y_0)$, $W_1 = Re(Y_1)$, $X_0 = Imq(Y_0)$ and $X_1 = Imq(Y_1)$.

The Bessel functions can now be expressed in the new notation as:

$$J_0(\xi, e^{j\phi}) = \left[U_0(\xi, e^{j(\pi-\phi)}) - j V_0(\xi, e^{j(\pi-\phi)})\right]$$

$$J_1(\xi, e^{j\phi}) = \left[-U_1(\xi, e^{j(\pi-\phi)}) + j V_1(\xi, e^{j(\pi-\phi)})\right] \qquad \text{(C-12)}$$

$$Y_0(\xi, e^{j\phi}) = \left[W_0(\xi, e^{j(\pi-\phi)}) + 2V_0(\xi, e^{j(\pi-\phi)})\right] - j\left[X_0(\xi, e^{j(\pi-\phi)}) - 2U_0(\xi, e^{j(\pi-\phi)})\right]$$

$$Y_1(\xi, e^{j\phi}) = \left[-W_1(\xi, e^{j(\pi-\phi)}) - 2V_1(\xi, e^{j(\pi-\phi)})\right] + j\left[X_1(\xi, e^{j(\pi-\phi)}) - 2U_1(\xi, e^{j(\pi-\phi)})\right]$$

$$K_0(\kappa_0 r_0) = \frac{\pi}{2}\left\{\left[-W_0(\xi, e^{j(\pi-\phi)}) - V_0(\xi, e^{j(\pi-\phi)})\right] + j\left[X_0(\xi, e^{j(\pi-\phi)}) - U_0(\xi, e^{j(\pi-\phi)})\right]\right\}$$

$$K_1(\kappa_0 r_0) = \frac{\pi}{2}\left\{\left[X_1(\xi, e^{j(\pi-\phi)}) - U_1(\xi, e^{j(\pi-\phi)})\right] + j\left[W_1(\xi, e^{j(\pi-\phi)}) + V_1(\xi, e^{j(\pi-\phi)})\right]\right\}$$

The real and imaginary terms of K_0 and K_1, are further defined (for simplicity) as:

$$Q_1(\xi, \pi-\phi) = \left[X_1(\xi, e^{j(\pi-\phi)}) - U_1(\xi, e^{j(\pi-\phi)})\right],$$

$$R_1(\xi, \pi-\phi) = \left[W_1(\xi, e^{j(\pi-\phi)}) + V_1(\xi, e^{j(\pi-\phi)})\right],$$

$$S_0(\xi, \pi-\phi) = \left[-W_0(\xi, e^{j(\pi-\phi)}) - V_0(\xi, e^{j(\pi-\phi)})\right] \text{ and}$$

$$T_0(\xi, \pi-\phi) = \left[X_0(\xi, e^{j(\pi-\phi)}) - U_0(\xi, e^{j(\pi-\phi)})\right]$$

Therefore, one can now write K_o and K_1 as

$$K_o = \frac{\pi}{2}\left[S_o(\xi, \pi-\phi) + j\, T_o(\xi, \pi-\phi)\right] \quad \text{and}$$

$$K_1 = \frac{\pi}{2}\left[Q_1(\xi, \pi-\phi) + j\, R_1(\xi, \pi-\phi)\right] \tag{C-13}$$

The right-hand side of Equation (C-8) is:

$$\frac{\beta_o K_1(\kappa_o r_o)}{\kappa_o K_o(\kappa_o r_o)} = \frac{\beta_o r_o e^{-j\theta}}{\xi} \frac{\left[(Q_1 S_o + R_1 T_o) - j(Q_1 T_o - R_1 S_o)\right]}{(S_o^2 + T_o^2)} \tag{C-14}$$

Let $C = \left[Q_1(\xi, \pi-\phi)\, S_o(\xi, \pi-\phi) + R_1(\xi, \pi-\phi)\, T_o(\xi, \pi-\phi)\right]$

and $D = \left[Q_1(\xi, \pi-\phi)\, T_o(\xi, \pi-\phi) - R_1(\xi, \pi-\phi)\, S_o(\xi, \pi-\phi)\right]$

Equation (C-14) can be written as: (C-15)

$$\frac{\beta_o K_1(\kappa_o r_o)}{\kappa_o K_o(\kappa_o r_o)} = \frac{\beta_o r_o}{\xi} \frac{\left[(C\cos(\theta) - D\sin(\theta)) - j(D\cos(\theta) + C\sin(\theta))\right]}{S_o^2(\xi, \pi-\phi) + T_o^2(\xi, \pi-\phi)}$$

Equating Equation (C-11) and Equation (C-15) gives:

$$\frac{-\beta}{\rho}\left[\frac{(A\sin(\varphi) + B\cos(\varphi)) + j(A\cos(\varphi) - B\sin(\varphi))}{U_o^2(\rho, \gamma) + V_o^2(\rho, \gamma)}\right] = \frac{\beta_o}{\xi}\left[\frac{(C\cos(\theta) - D\sin(\theta)) - j(D\cos(\theta) + C\sin(\theta))}{S_o^2(\xi, \pi-\phi) + T_o^2(\xi, \pi-\phi)}\right] \tag{C-16}$$

Separating Equation (C-16) into real and imaginary parts gives:

$$\frac{\beta_o}{\beta} = \frac{-\xi}{\rho} \frac{\left[S_o^2(\xi, \pi-\phi) + T_o^2(\xi, \pi-\phi)\right]\left[A\sin(\varphi) + B\cos(\varphi)\right]}{\left[U_o^2(\rho, \varphi) + V_o^2(\rho, \varphi)\right]\left[C\cos(\theta) - D\sin(\theta)\right]} \tag{C-17}$$

and $$\frac{\left[A\cos(\varphi) - B\sin(\varphi)\right]}{\left[A\sin(\varphi) + B\cos(\varphi)\right]} = -\frac{\left[D\cos(\theta) + C\sin(\theta)\right]}{\left[C\cos(\theta) - D\sin(\theta)\right]} \tag{C-18}$$

Equation (C-18) is the transcendental root equation.